

The distribution of the moment of inertia for harmonically trapped noninteracting Bosons at finite temperature: large deviations

Manas Kulkarni^{1*}, Satya N. Majumdar^{2†} and Gr  gory Schehr^{3  }

1 International Centre for Theoretical Sciences, Tata Institute of Fundamental Research,
Bangalore 560089, India

2 LPTMS, CNRS, Univ. Paris-Sud, Université Paris-Saclay, 91405 Orsay, France

3 Sorbonne Université, Laboratoire de Physique Théorique et Hautes Energies, CNRS
UMR 7589, 4 Place Jussieu, 75252 Paris Cedex 05, France

* manas.kulkarni@icts.res.in † satyanarayan.majumdar@cnrs.fr ‡ gregory.schehr@lpthe.jussieu.fr

Abstract

We compute the full probability distribution of the moment of inertia $I \propto \sum_{i=1}^N \vec{r}_i^2$ of a gas of N noninteracting bosons trapped in a harmonic potential $V(r) = (1/2) m \omega^2 r^2$, in all dimensions and at all temperature. The appropriate thermodynamic limit in a trapped Bose gas consists in taking the limit $N \rightarrow \infty$ and $\omega \rightarrow 0$ with their product $\rho = N\omega^d$ fixed, where ρ plays the role analogous to the density in a translationally invariant system. In this thermodynamic limit and in dimensions $d > 1$, the harmonically trapped Bose gas undergoes a Bose-Einstein condensation (BEC) transition as the density ρ crosses a critical value $\rho_c(\beta)$, where β denotes the inverse temperature. We show that the probability distribution $P_\beta(I, N)$ of I admits a large deviation form $P_\beta(I, N) \sim e^{-V\Phi(I/V)}$ where $V = \omega^{-d} \gg 1$. We compute explicitly the rate function $\Phi(z)$ and show that it exhibits a singularity at a critical value $z = z_c$ where its second derivative undergoes a discontinuous jump. We show that the existence of such a singularity in the rate function is directly related to the existence of a BEC transition and it disappears when the system does not have a BEC transition as in $d \leq 1$. An interesting consequence of our results is that even if the actual system is in the fluid phase, i.e., when $\rho < \rho_c(\beta)$, by measuring the distribution of I and analysing the singularity in the associated rate function, one can get a signal of the BEC transition in $d > 1$. This provides a real space diagnostic for the BEC transition in the noninteracting Bose gas.

Contents

1	Introduction	2
2	Model and the observable of interest	4
3	The partition function $Z(N, \beta)$ at large N	8
3.1	The fluid phase $\rho < \rho_c(\beta)$: when there is a saddle point	10
3.2	The condensed phase $\rho > \rho_c(\beta)$: when there is no saddle point	11
3.3	Connecting the fluid and the condensed phase on a smaller scale of $(\rho - \rho_c(\beta)) \sim O(1/\sqrt{V})$	12

4 Statistics of the moment of inertia	14
4.1 Computation of $\Psi(\lambda)$	16
4.1.1 The F-F phase	17
4.1.2 The F-C phase	19
4.1.3 The C-F and the C-C phases	20
4.2 Computation of the rate function $\Phi(z)$	21
4.2.1 The limit $z \rightarrow \infty$	22
4.2.2 The limit $z \rightarrow 0$	22
4.2.3 The limit $z \rightarrow z_{\min}$	23
4.2.4 The limit $z \rightarrow z_c$	23
5 Conclusion	24
6 Acknowledgments	25
A Duality relation in d dimensions	26
B Mean and variance of I	27
C The computation of a multidimensional integral	28
References	28

1 Introduction

Recent advances in the experimental techniques in cold atom systems have made it possible to explore the spatial distribution of quantum particles, bosons and fermions, in the presence of a confining trap with or without interactions between the particles [1–16]. The presence of a trap breaks the translational symmetry and makes the system inhomogeneous in space. In the absence of interactions, the energy spectrum of such systems is trivial and consist of filling up the single particle energy levels with the appropriate Bose or Fermi statistics. In other words, the many-body Hamiltonian is trivially quadratic in the second quantised formalism. However, the spatial distributions of such quantum particles is still nontrivial in such noninteracting systems, due to the fact that the many-body wave functions in real space can be rather complicated due to the statistics of the particles. For instance, for fermions, the Pauli exclusion principle forbids two fermions (with the same spin) to be in the same position in space or equivalently, any many-body eigenfunction must have a Slater determinant form, which ensures antisymmetry under the exchange of a pair of fermions. Similarly, for bosons, the many-body eigenfunction must have a permanental form, ensuring the symmetry under the exchange of any pair of bosons. It is also interesting to explore the dependence of these spatial properties on the temperature. For instance for fermions, physical observables exhibit “quantum behaviors” when the temperature is much less than the Fermi energy, while at a higher temperature, they behave more or less classically. For bosonic systems, on the other hand, there is a Bose-Einstein condensation (BEC) at a critical temperature $T_c > 0$ in dimensions $d > d_c$ (where d_c denotes the lower critical dimension that depends on the geometry of the confining potential). For example, for a hard-box potential $d_c = 2$, while for a harmonic trap $d_c = 1$ [12]. This means that a macroscopically large fraction of bosons condense in the single-particle ground state for

$T < T_c$ (equivalently when the density exceeds a critical value ρ_c). While the mechanism behind the BEC transition for noninteracting bosons is very simple in the energy space, it is not completely evident how, by inspecting a configuration of bosons in real space, one can get a marked signal for the existence or not of the thermodynamic BEC transition. The results of most experimental measurements are reported in momentum space and, in fact, there have been relatively few experiments reporting the manifestation of BEC in real space [17, 18].

In most of the experimental systems, the number of bosons N is conserved. Hence the natural ensemble to study is the canonical one, where one is interested in the canonical partition function $Z(N, \beta)$ where β is the inverse temperature. However, computing $Z(N, \beta)$ and extracting its large N behavior is somewhat cumbersome even for noninteracting bosons and, hence, in most textbooks (see e.g. [19–21]), one usually studies the grand-canonical ensemble where the number of particles is allowed to fluctuate around its average value. Theoretically it is easier to study the grand-canonical partition function, which is simply the generating function of the canonical partition function $Z(N, \beta)$. However, extracting the precise asymptotic behaviours of $Z(N, \beta)$ for large N from its generating function is not that straightforward, especially when the system undergoes a BEC phase transition. Moreover, even if one could extract the large N behavior of $Z(N, \beta)$ explicitly, it does not directly provide any information about the spatial configurations of bosons that we are interested in. This is due to the fact that $Z(N, \beta)$, for noninteracting bosons, depends only on the single-particle energies ϵ_i 's and, hence, does not carry any information on the spatial properties of the systems, since it does not involve the many-body eigenfunctions that encode the spatial distribution.

There have been recent progresses in characterising the spatial properties of noninteracting fermions in a trap (harmonic or otherwise), both at zero and finite temperature and several spatial observables have been computed explicitly. This includes the probability distribution induced by quantum and thermal fluctuations of the position of the farthest fermion from the center of the trap, the full counting statistics, etc [22–25] (see e.g. [26] for a review). In this paper, we are interested in a particular spatial observable, namely the distribution of the moment of inertia of the trapped noninteracting particles at arbitrary temperature and in arbitrary dimension. The moment of inertia I is simply defined as the linear statistics

$$I \propto \sum_{i=1}^N \vec{r}_i^2, \quad (1)$$

where \vec{r}_i denotes the position of the i -th particle in d dimensions. For noninteracting fermions in a harmonic trap, and only in $d = 1$, the distribution of I was exactly computed at all temperatures [27] and it displays nontrivial large deviation behaviors with a rate function that depends explicitly on temperature and displays quite different behaviors in the quantum (where temperature T is of the order of the gap in the single particle energy spectrum) and the classical regime (where the temperature is of the order of the Fermi energy). It is then natural to ask how this distribution of I behaves for noninteracting Bosons in a trap. In particular, for $d > d_c$, where the system undergoes a BEC transition, how does this transition affect the statistics of I ?

In this paper, we address this question and compute exactly the probability distribution of I given in Eq. (1) for noninteracting bosons in a harmonic trap in all dimensions and all temperature. This exact computation is possible by using an interesting identity that relates the cumulant generating function of I with the partition function $Z(N, \beta)$. This identity was derived and used before to compute the finite temperature properties of the distribution of I for noninteracting fermions in a harmonic trap in one dimension [27]. Here we show that this identity is more general and can be applied for bosons as well.

Moreover, we show that this identity holds even in higher dimensions and at any temperature. Consequently, it gives us access to the cumulant generating function of I and, in turn, to its full distribution at any temperature and in any dimension. This observable is a natural one that provides some spatial information about the positions of the bosons and, in principle, is also measurable in experiments that record real-space images of bosons using a quantum microscope [28–32]. For example, one just needs to have many samples of the Bose gas in real space. From each sample, one can compute I using Eq. (1) and then obtain a histogram of I . Our theoretical predictions for the distribution of I for noninteracting bosons in a trap can then be used as a benchmark to compare such possible experimental data, since in real systems the bosons are typically interacting.

Let us briefly summarise our main results. We consider N noninteracting bosons in a harmonic trap $V(r) = (1/2)m\omega^2\vec{r}^2$ in d dimensions. The appropriate thermodynamic limit corresponds to taking $N \rightarrow \infty$ and $\omega \rightarrow 0$ keeping $\rho = N\omega^d$ fixed. In this thermodynamic limit, the system undergoes the BEC transition for $d > d_c = 1$ across the critical density

$$\rho_c(\beta) = \frac{\zeta(d)}{\beta^d}, \quad (2)$$

where $\zeta(n) = \sum_{k \geq 1} 1/k^n$ is the Riemann zeta function (with $n > 1$) and β denotes the inverse temperature. For $\rho < \rho_c(\beta)$, the system is in the fluid phase, while for $\rho > \rho_c(\beta)$ it has a condensate. We compute exactly the distribution $P_\beta(I, N)$ of the moment of inertia I in the thermodynamic limit and show that it admits a large deviation form

$$P_\beta(I, N) \approx e^{-V\Phi(\frac{I}{V})}, \quad (3)$$

where $V = \omega^{-d} \gg 1$ is a large parameter and $\Phi(z)$ denotes the rate function associated to the distribution of I . We show that, whenever the system of bosons exhibits a BEC transition in the thermodynamic limit (e.g., when $d > 1$), the rate function $\Phi(z)$ associated with I has a singularity at a critical point z_c where its second derivative is discontinuous. If there is no BEC transition (e.g., in $d = 1$), the rate function $\Phi(z)$ becomes an analytical function with no singularity. Thus, by measuring the distribution of I , one can detect if the system undergoes a BEC transition or not.

The rest of the paper is organised as follows. In Section 2, we introduce the model precisely and derive the identity that relates the cumulant generating function of I with the canonical partition function $Z(N, \beta)$. In Section 3 we derive the large N asymptotic behaviour of $Z(N, \beta)$ in any dimension and show that, for $d > 1$, it does have a BEC transition in the thermodynamic limit. These large N asymptotics of $Z(N, \beta)$ are then used in Subsection 4.1 to derive the cumulant generating function of I , using the identity established in Section 2. In Subsection 4.2, we extract the rate function $\Phi(z)$ from the cumulant generating function and derive in particular its nonanalytic behavior at the critical point $z = z_c$. We conclude with a summary and outlook in Section 5. Some details of the computations are relegated to the three appendices.

2 Model and the observable of interest

We consider a system of N noninteracting bosons in a harmonic trap in dimension d . The Hamiltonian of the system is given by

$$\hat{H}_N(m) = \sum_{i=1}^N \hat{h}_i(m) \quad \text{where} \quad \hat{h}_i(m) = \frac{\vec{p}_i^2}{2m} + \frac{1}{2}m\omega^2\vec{r}_i^2, \quad (4)$$

where m is the mass of the particles and ω is the frequency of the trap. Here \vec{p}_i and \vec{r}_i denote respectively the position and the momentum of particle i in dimension d . This is slightly different from the ideal Bose gas in a box of linear size L , which is a textbook example. There, in the thermodynamic limit, where $N \rightarrow \infty$, $L \rightarrow \infty$ but with the ratio $\rho = N/L^d$ fixed, it is well known [19–21] that the system undergoes a condensation transition – the celebrated Bose-Einstein condensation (BEC) – when the density ρ exceeds a critical value ρ_c at a fixed temperature, or equivalently when the temperature goes below a critical temperature T_c for a fixed density. For $\rho < \rho_c$ the system is in a “fluid” phase, while for $\rho > \rho_c$, it is in a “condensed” phase where an extensive number of Bosons condense in the single-particle ground state. For the box geometry, this happens for any dimension $d > 2$ [20, 21]. In contrast, for a harmonically trapped Bose gas, there is no confining volume. Indeed, from Eq. (4), it is clear that $1/\omega$, which typically denotes the width of the potential, plays an analogous role as the size L in the box geometry. Hence, in this case $V = 1/\omega^d$ is the analogue of the volume in the box geometry. Consequently the thermodynamic limit here corresponds to taking the limit $N \rightarrow \infty$, $\omega \rightarrow 0$ but keeping the product

$$\rho = N\omega^d , \quad (5)$$

fixed (see e.g. [33]). Henceforth we will call this product ρ as the “density”. As in the box geometry, there is a BEC transition in the harmonic case also, as one increases the density ρ through a critical density $\rho_c(\beta)$ for a fixed inverse temperature β (alternatively reducing the temperature through a critical temperature T_c for a fixed density). However, in contrast to the box case, the BEC transition in the harmonic case occurs for any dimension $d > 1$ [12].

Our goal in this paper is to compute the statistics of the observable

$$I = m\omega^2 \sum_{i=1}^N \vec{r}_i^2 , \quad (6)$$

at any temperature T and density ρ for a harmonically trapped ideal Bose gas. This observable represents twice the potential energy of the Bose gas defined in Eq. (4). We will show that the harmonic case allows an exact solution for the distribution of I in the thermodynamic limit. The distribution of I is defined as follows. Consider N noninteracting Bosons at a fixed total energy E . The system is fully specified in real space provided we know the many-body bosonic eigenfunction $\Psi_E(\vec{r}_1, \dots, \vec{r}_N)$, normalized to unity. Here \vec{r}_i represents the positon of the i -th Boson. By definition, $|\Psi_E(\vec{r}_1, \dots, \vec{r}_N)|^2$ represents the quantum joint probability density arising purely from quantum fluctuations at a fixed energy E . Of course the energy itself fluctuates at a fixed temperature. In the canonical ensemble where the temperature T and the number of bosons N is fixed, both the quantum and thermal fluctuations are captured by the joint probability density function (JPDF)

$$P_\beta(\vec{r}_1, \dots, \vec{r}_N) = \frac{1}{Z(N, \beta)} \sum_E e^{-\beta E} |\Psi_E(\vec{r}_1, \dots, \vec{r}_N)|^2 . \quad (7)$$

Here the partition function $Z(N, \beta)$ ensures the normalization of the JPDF and $\beta = 1/T$ represents the inverse temperature. The total energy E can be conveniently expressed in terms in the occupation numbers $n_{\vec{j}} = 0, 1, 2, \dots$ of the single-particle energy levels $\epsilon_{\vec{j}}$ labeled by the d -dimensional vector $\vec{j} = (j_1, \dots, j_d)$ and given by

$$\epsilon_{\vec{j}} = \left(j_1 + j_2 + \dots + j_d + \frac{d}{2} \right) \hbar\omega , \quad (8)$$

where j_i 's are nonnegative integers. The total energy E of a many-body state and the total number of particles can be expressed in terms of the occupation numbers $n_{\vec{j}}$'s

$$E = \sum_{\vec{j}} n_{\vec{j}} \epsilon_{\vec{j}} \quad , \quad N = \sum_{\vec{j}} n_{\vec{j}} . \quad (9)$$

The canonical partition function $Z(N, \beta)$ is then given by

$$Z(N, \beta) = \sum_E e^{-\beta E} = \sum_{\{n_{\vec{j}}\}} e^{-\beta \sum_{\vec{j}} n_{\vec{j}} \epsilon_{\vec{j}}} \delta_{\sum_{\vec{j}} n_{\vec{j}}, N} . \quad (10)$$

Taking the generating function with respect to (w.r.t.) N one finds

$$\sum_{N \geq 1} z^N Z(N, \beta) = \prod_{\vec{j}} \frac{1}{1 - z e^{-\beta \epsilon_{\vec{j}}}} , \quad (11)$$

where the product runs over all possible vectors $\vec{j} = (j_1, \dots, j_d)$ where j_i 's are nonnegative integers. Clearly the ground state corresponds to $\vec{j} = \vec{0} = (0, 0, \dots, 0)$. Inverting Eq. (11) formally, using Cauchy's formula, gives

$$Z(N, \beta) = \oint \frac{dz}{2\pi i} \frac{1}{z^{N+1}} \prod_{\vec{j}} \frac{1}{1 - z e^{-\beta \epsilon_{\vec{j}}}} , \quad (12)$$

where the contour integral over z runs over a circle centered at $z = 0$. Making further the change of variable $z = e^{-s}$ one can convert it to a Bromwich integral in the complex s -plane, namely

$$Z(N, \beta) = \int_{\Gamma} \frac{ds}{2\pi i} e^{sN} \frac{1}{1 - e^{-s-\beta \epsilon_{\vec{0}}}} e^{-\sum_{\vec{j} \neq \vec{0}} \ln(1 - e^{-s-\beta \epsilon_{\vec{j}}})} , \quad (13)$$

where we have separated out the contribution from the ground state with energy

$$\epsilon_{\vec{0}} = \hbar \omega \frac{d}{2} , \quad (14)$$

corresponding to $j_1 = j_2 = \dots = j_d = 0$. In Eq. (13), the Bromwich contour Γ runs vertically along the imaginary axis whose real part lies to the right of all the singularities of the integrand.

Given the joint distribution at finite inverse temperature β given in Eq. (7), the probability distribution of the linear statistics I defined in Eq. (6) can be expressed as

$$P_{\beta}(I, N) = \int d\vec{r}_1 \dots \int d\vec{r}_N P_{\beta}(\vec{r}_1, \dots, \vec{r}_N) \delta \left(I - m \omega^2 \sum_{i=1}^N \vec{r}_i^2 \right) . \quad (15)$$

Taking the Laplace transform w.r.t. I gives

$$\begin{aligned} \tilde{P}_{\beta}(\lambda, N) &= \int_0^{\infty} e^{-\lambda I} P_{\beta}(I, N) dI = \int d\vec{r}_1 \dots \int d\vec{r}_N P_{\beta}(\vec{r}_1, \dots, \vec{r}_N) e^{-\lambda m \omega^2 \sum_{i=1}^N \vec{r}_i^2} \\ &= \frac{1}{Z(N, \beta)} \sum_E e^{-\beta E} \int d\vec{r}_1 \dots \int d\vec{r}_N |\Psi_E(\vec{r}_1, \dots, \vec{r}_N)|^2 e^{-\lambda m \omega^2 \sum_{i=1}^N \vec{r}_i^2} . \end{aligned} \quad (16)$$

where we used the explicit expression of $P_{\beta}(\vec{r}_1, \dots, \vec{r}_N)$ in Eq. (7). In general, this multi-dimensional integral is hard to perform explicitly, since the many-body wave function of

an excited state E is a permanent of the associated single-particle eigenfunctions (each of them being the product of a Gaussian and d Hermite polynomials for each coordinate). Moreover, summing over all possible energies E makes the evaluation of $\tilde{P}_\beta(\lambda, N)$ in Eq. (16) rather daunting. To circumvent this problem, we make use of a nontrivial identity, which was first derived for one-dimensional noninteracting fermions in [27] by a rather complicated method. Here, we first rederive this identity by a much simpler method that demonstrates its generality, namely that it is valid in all dimensions and at all temperatures, irrespective of the statistics of the particles, i.e., it holds for both fermions and bosons. In Appendix A we provide a simple proof of this identity which reads

$$\tilde{P}_\beta(\lambda, N) = \langle e^{-\lambda m \omega^2 \sum_{i=1}^N \vec{r}_i^2} \rangle = \frac{Z(N, \tilde{\beta}(\lambda))}{Z(N, \beta)}, \quad (17)$$

where $Z(N, \beta)$ is the canonical partition function given in Eq. (13) and $\tilde{\beta}(\lambda)$ is determined from the exact relation

$$\cosh(\tilde{\beta}(\lambda)\hbar\omega) = \cosh(\beta\hbar\omega) + \lambda\hbar\omega \sinh(\beta\hbar\omega). \quad (18)$$

Note that when $\lambda = 0$, we have $\tilde{\beta}(0) = \beta$. This identity relates the statistics of I to the partition function $Z(N, \beta)$ in Eq. (13), the computation of which does not require any knowledge of the many-body eigenfunction $\Psi_E(\vec{r}_1, \dots, \vec{r}_N)$. Hence, thanks to this identity (17), the statistics of the operator I depend only on the spectrum of \hat{H}_N (i.e., its energy eigenvalues) but not on its eigenfunctions. We call this identity in Eqs. (17) and (18) a duality relation as it involves partition functions at two different temperatures.

Given this relation (17), one can compute any moments of I by taking repeated derivatives of (17) w.r.t. λ and setting $\lambda = 0$. For example, the average $\langle I \rangle$ is simply given by

$$\langle I \rangle = -\frac{\partial}{\partial \lambda} \langle e^{-\lambda I} \rangle \Big|_{\lambda=0}. \quad (19)$$

Taking the derivative of Eq. (17) w.r.t. λ and using the relation (18) and setting $\lambda = 0$ gives the exact relation

$$\langle I \rangle = -\frac{\partial \ln Z(N, \beta)}{\partial \beta}. \quad (20)$$

The right hand side represents just the average energy of the system (up to a factor $1/m$). This is expected since, for the harmonic oscillator, the kinetic part and the potential part of the total energy have identical behaviors (since the position \vec{r}_i and the momentum \vec{p}_i play a symmetric role in the Hamiltonian). Hence the average total energy is twice that of the potential energy and hence coincides with the average value of the observable $I = m\omega^2 \sum_{i=1}^N \vec{r}_i^2$.

Similarly, by taking two derivatives of Eq. (17) w.r.t. λ , one can relate the variance of I to the partition function as follows (for a detailed derivation, see Appendix B)

$$\text{Var}(I) = \langle I^2 \rangle - \langle I \rangle^2 = \left[\frac{\partial^2 \ln Z}{\partial \beta^2} + \hbar\omega \coth(\beta\hbar\omega) \langle I \rangle \right]. \quad (21)$$

Note that the first term on the right hand side is exactly the specific heat of the system, while the second term represents a quantum correction.

We thus see from Eq. (17) that computing the full distribution $P_\beta(I, N)$ requires the knowledge of the exact partition function $Z(N, \beta)$ as a function of β for a given N . Analysing the partition function $Z(N, \beta)$ for finite N turns out to be rather hard. However, in the next section, we show that we can make progress in the appropriate large N limit mentioned in Eq. (5). Namely we will take the limits $N \rightarrow \infty$ and $V = 1/\omega^d \rightarrow \infty$, but keeping the ratio $\rho = N/V = N\omega^d$ fixed.

3 Large N analysis of the partition function $Z(N, \beta)$

For simplicity, we will henceforth use units in which $m = 1$ and $\hbar = 1$. Our starting point is the exact expression for $Z(N, \beta)$ in Eq. (13) which is valid for arbitrary N . We first rewrite this expression as

$$Z(N, \beta) = \int_{\Gamma} \frac{ds}{2\pi i} \frac{1}{1 - e^{-s - \beta\epsilon_0}} e^{Ns - g_N(\beta, s)} , \quad g_N(\beta, s) = \sum_{\vec{j} \neq \vec{0}} \ln(1 - e^{-s - \beta\epsilon_{\vec{j}}}) . \quad (22)$$

In the scaling limit $\omega \rightarrow 0$, one can replace the sum in $g_N(\beta, s)$ by an integral. This is done as follows. We first define the variables

$$k_i = \beta\omega j_i , \quad (23)$$

where j_i 's are non-negative integers. In the limit $\omega \rightarrow 0$, the k_i 's become essentially continuous variables with increment $\Delta k_i = \beta\omega \rightarrow 0$. Therefore, multiplying and dividing $g_N(\beta, s)$ in Eq. (22) by $(\beta\omega)^d$, we can replace the sum by a d -dimensional integral (valid in the limit $\omega \rightarrow 0$)

$$g_N(\beta, s) \approx \frac{1}{(\beta\omega)^d} \int_{>} d\vec{k} \ln(1 - e^{-s - k}) = \frac{V}{\beta^d} \int_{>} d\vec{k} \ln(1 - e^{-s - \sum_{i=1}^d k_i}) , \quad (24)$$

where $V = 1/\omega^d$ is a fixed number of order $O(1)$, as mentioned in Eq. (5). The integral in Eq. (24) runs over the “first quadrant” in the d -dimensional Fourier space, i.e., over $k_i \geq 0$, as indicated by the notation $\int_{>} d\vec{k}$. Furthermore, in the limit $\beta\omega \rightarrow 0$, the term in the integrand representing the contribution from the ground state reduces simply to $1/(1 - e^{-s - \beta\epsilon_0}) \approx 1/(1 - e^{-s})$. Therefore in this limit, using $N = \rho V$, the partition function reduces to

$$Z(N, \beta) = \int_{\Gamma} \frac{ds}{2\pi i} \frac{1}{1 - e^{-s}} e^{VA(s, \rho)} , \quad A(s, \rho) = s\rho - \frac{1}{\beta^d} \int d\vec{k} \ln(1 - e^{-s - \sum_{i=1}^d k_i}) . \quad (25)$$

Before proceeding, let us make an important remark: the integrand in the expression of $Z(N, \beta)$ in Eq. (25) has a pole at $s = 0$ arising from the ground state contribution. Hence the real part of the Brownich contour must be at $s > 0$. The structure of the integral clearly suggests to look for a saddle point solution on the real axis at $s = s^* > 0$. Setting $\partial A/\partial s = 0$ at $s = s^*$ one gets the saddle point equation

$$\rho = \frac{1}{\beta^d} \int_{>} d\vec{k} \frac{1}{e^{s^* + \sum_{i=1}^d k_i} - 1} . \quad (26)$$

The integral on the right hand side can be performed explicitly in d dimensions and it leads to (see Appendix C)

$$\tilde{\rho} = \rho \beta^d = \frac{1}{\Gamma(d)} \int_0^{\infty} dq q^{d-1} \frac{1}{e^{s^* + q} - 1} = h_d(s^*) \equiv \text{Li}_d(e^{-s^*}) , \quad \text{where} \quad \text{Li}_n(z) = \sum_{k=1}^{\infty} \frac{z^k}{k^n} . \quad (27)$$

The function $h_d(s) \equiv \text{Li}_d(e^{-s})$ is a monotonically decreasing function of s (see Fig. 1 for $d = 3$) with asymptotic behaviors given by

$$h_d(s) \approx \begin{cases} \zeta(d) & , \quad s \rightarrow 0 \\ e^{-s} & , \quad s \rightarrow \infty . \end{cases} \quad (28)$$

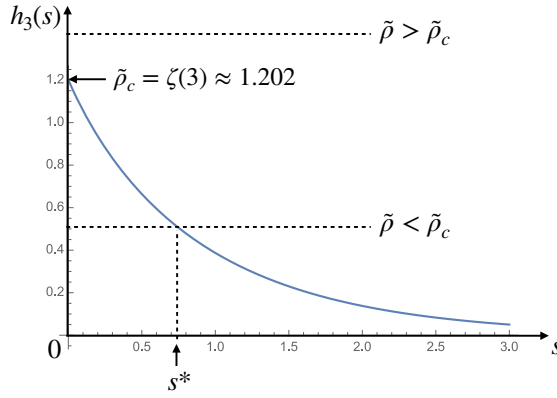


Figure 1: The solid blue line is a plot of the function $h_{d=3}(s) = \text{Li}_{d=3}(e^{-s})$ given in Eq. (27) as a function of s . The value at $s = 0$, namely $h_{d=3}(s = 0) = \zeta(3)$, denotes the critical density $\tilde{\rho}_c$. The two horizontal lines indicates two representative values of the density $\tilde{\rho}$: one in the fluid phase ($\tilde{\rho} < \tilde{\rho}_c$) and the other in the condensed phase (where $\tilde{\rho} > \tilde{\rho}_c$). In the fluid phase, given the density $\tilde{\rho} < \tilde{\rho}_c$, there is a unique value s^* such that $h_{d=3}(s^*) = \tilde{\rho}$ as shown in the figure. This shows that, in the fluid phase, there is a nonzero value $s = s^*$ where a saddle point occurs. As $\tilde{\rho}$ approaches $\tilde{\rho}_c$ from below, the saddle point s^* approaches to 0.

Thus the saddle point s^* is given by the positive root of $h_d(s^*) = \tilde{\rho}$. Since $h_d(s)$ is a monotonically decreasing function of s , its maximum value for nonnegative s occurs at $s = 0$, with the value $h_d(0) = \zeta(d)$. We note that $\zeta(d)$ is finite only for $d > 1$. For $d \leq 1$, $h_d(s) \rightarrow +\infty$ as $s \rightarrow 0$. Thus for $d \leq 1$, there will always be a saddle point solution $s^* > 0$. In contrast, for $d > 1$, a saddle point solution may or may not exist, depending on the value of $\tilde{\rho} = \rho\beta^d$, which is our control parameter. For $d > 1$, since $h_d(0) = \zeta(d)$ is finite, there will be a saddle point solution $s^* > 0$ provided $\tilde{\rho} < \tilde{\rho}_c$ (see Fig. 1 for an illustration in $d = 3$) where

$$\tilde{\rho}_c = \zeta(d) . \quad (29)$$

This defines a critical line $\rho\beta^d = \zeta(d)$ in the (ρ, β) plane across which the BEC occurs. This critical line can be traversed either by changing ρ at fixed β or by changing β at fixed ρ . Below, for convenience, we will vary ρ through this critical line, with β fixed. In this case the critical density $\rho_c(\beta)$ is given by

$$\rho_c(\beta) = \frac{\zeta(d)}{\beta^d} . \quad (30)$$

As ρ approaches $\rho_c(\beta)$ from below, the saddle point $s^* \rightarrow 0$ (see Fig. 2). For $\rho > \rho_c(\beta)$, there is thus no saddle point and one has to evaluate the Bromwich integral along the imaginary axis passing through $s \rightarrow 0^+$. Thus for $d > 1$, as one varies ρ through the critical value $\rho_c(\beta)$ the system undergoes a transition. We will see later that the phase $\rho < \rho_c(\beta)$ where there is a positive saddle point $s^* > 0$, corresponds to the so called “fluid” phase. In contrast, for $\rho > \rho_c(\beta)$ when there is no saddle point, the system is in a Bose-Einstein condensed (BEC) phase.

For later purposes we note that the action $A(s, \rho)$ in Eq. (25) can also be evaluated explicitly by performing the integral over \vec{k} (see Appendix C), leading to

$$A(s, \rho) = \rho s + \frac{1}{\beta^d} \text{Li}_{d+1}(e^{-s}) . \quad (31)$$

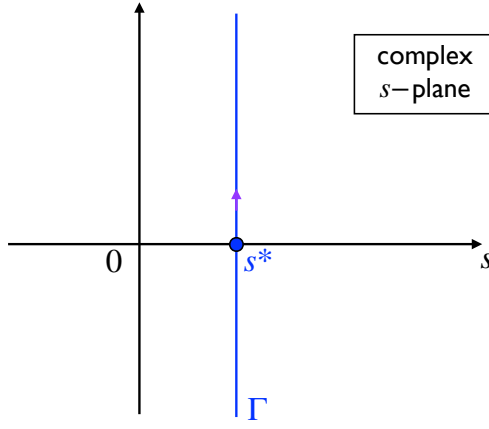


Figure 2: The vertical blue line denotes the Bromwich contour Γ in the complex s -plane in Eq. (25). The Bromwich contour intersects the real axis at $s = s^*$ denoting the location of the saddle point in Eq. (27).

We will focus here only on $d > 1$ when there is a condensation transition, as argued above, at a critical density $\rho = \rho_c(\beta) = \zeta(d)/\beta^d$. For later purposes, it will also be useful to extract the small s expansion of $A(s, \rho)$ in Eq. (31). It turns out that this small s expansion of $A(s, \rho)$ has both a regular and a singular part. The singular part depends on whether d is an integer or not. For noninteger $d > 1$, it reads

$$A(s, \rho) = \left[\frac{1}{\beta^d} \zeta(d+1) + (\rho - \rho_c(\beta)) s + \frac{1}{\beta^d} \zeta(d-1) s^2 + \dots \right] + \frac{\Gamma(-d)}{\beta^d} s^d + \dots \quad (32)$$

where the square brackets indicate the regular part of the expansion, while $\Gamma(-d) s^d$ is the leading singular term in the small s expansion. For integer $d > 1$, while the regular part remains the same, the leading singular part is different and one gets

$$A(s, \rho) = \left[\frac{1}{\beta^d} \zeta(d+1) + (\rho - \rho_c(\beta)) s + \frac{1}{\beta^d} \zeta(d-1) s^2 + \dots \right] + \frac{(-1)^{d+1}}{\beta^d \Gamma(d+1)} s^d \ln s + \dots \quad (33)$$

In the large V limit, it turns out that the singular terms give rise to only subleading corrections to the leading large V behavior of $Z(N, \beta)$ in Eq. (25), as will be discussed shortly.

3.1 The fluid phase $\rho < \rho_c(\beta)$: when there is a saddle point

As discussed above, in this case there is a saddle point which is obtained by minimizing the action $A(s, \rho)$ in Eq. (25) as a function of s for a fixed $\rho < \rho_c(\beta)$ (and fixed β). This leads to the explicit saddle point equation (27) which can then be used to obtain $s^*(\rho)$ by inverting the relation

$$\text{Li}_d(e^{-s^*}) = \rho \beta^d. \quad (34)$$

Substituting this value of s^* in the action $A(s, \rho)$ in Eq. (31) gives $A(s^*(\rho), \rho)$. Consequently, evaluating the partition function in Eq. (25) for large N , we get

$$\frac{\ln Z(N, \beta)}{V} \xrightarrow[V \rightarrow \infty]{} A(s^*(\rho), \rho) = \rho s^* + \frac{1}{\beta^d} \text{Li}_{d+1}(e^{-s^*}), \quad (35)$$

where we have used the explicit expression of $A(s, \rho)$ from Eq. (31). Even though this result is valid for all $\rho < \rho_c(\beta)$ in the fluid phase, one can obtain a more explicit expression

for $Z(N, \beta)$ in the vicinity of the critical point, i.e., when ρ approaches $\rho_c(\beta)$ from below. As $\rho \rightarrow \rho_c(\beta)$ the saddle point $s^*(\rho) \rightarrow 0$ in Fig. 2. In this limit, it is easy to show that the action $A(s^*, \rho)$ in (35) behaves quadratically as a function of $(\rho - \rho_c(\beta))$ for small $(\rho - \rho_c(\beta))$ (see Fig. 3), namely

$$\frac{\ln Z(N, \beta)}{V} \xrightarrow[V \rightarrow \infty]{} A(s^*, \rho) \approx \frac{\zeta(d+1)}{\beta^d} - \frac{\beta^d}{4\zeta(d-1)}(\rho_c(\beta) - \rho)^2. \quad (36)$$

The same result can also be obtained more easily by first expanding $A(s, \rho)$ for small s as in Eq. (32) or (33) and then minimizing with respect to s .

3.2 The condensed phase $\rho > \rho_c(\beta)$: when there is no saddle point

As mentioned before, when ρ approaches $\rho_c(\beta)$ from below, the saddle point $s^* \rightarrow 0$. We recall that, since the integrand in Eq. (25) has a pole as $s = 0$, the real part of the Bromwich contour can not cross $s = 0$. Hence one has to analyse the integral in Eq. (25) along a contour that passes just to the right of $s = 0$. In other words, we need to use the small s expansion of $A(s, \rho)$ in Eq. (32) or (33) and then analyse the integral, but without the existence of a saddle point. In fact, from the small s expansion in Eq. (32) or (33), it is clear that the function $A(s, \rho)$ has a minimum at $s = s^*$ only for $\rho < \rho_c(\beta)$. For $\rho > \rho_c(\beta)$ and using the $s \rightarrow 0$ expansion of $A(s, \rho)$ in Eq. (32) or (33), we first rewrite the expression of the partition function as

$$Z(N, \beta) \approx e^{V \frac{\zeta(d+1)}{\beta^d}} \int_{\Gamma} \frac{ds}{2\pi i} \frac{1}{s} e^{V(\rho - \rho_c(\beta))s + \frac{\zeta(d-1)}{\beta^d} V s^2 + \dots}. \quad (37)$$

Consider now $(\rho - \rho_c(\beta)) \sim O(1)$, while $V \rightarrow \infty$. In this scale, by rescaling $sV = \tilde{s}$, we see that only the leading term inside the exponential survives (all higher order terms, including the quadratic one vanishes in this limit). This leads to

$$Z(N, \beta) \approx e^{V \frac{\zeta(d+1)}{\beta^d}} \int_{\Gamma} \frac{d\tilde{s}}{2\pi i} \frac{1}{\tilde{s}} e^{(\rho - \rho_c(\beta))\tilde{s}} = e^{V \frac{\zeta(d+1)}{\beta^d}} \theta(\rho - \rho_c(\beta)), \quad (38)$$

where we used the fact that the integral over \tilde{s} is simply $\theta(\rho - \rho_c(\beta))$, with $\theta(x)$ denoting the Heaviside step function. This relation (38) can be proved by first taking a derivative with respect to $\rho - \rho_c(\beta)$, which gives $\delta(\rho - \rho_c(\beta))$ and then integrating it back. This gives, in the condensed phase where $(\rho - \rho_c(\beta)) > 0$ and is $O(1)$

$$\frac{\ln Z(N, \beta)}{V} \xrightarrow[V \rightarrow \infty]{} \frac{\zeta(d+1)}{\beta^d}. \quad (39)$$

Thus this leading order behavior is independent of $\rho - \rho_c(\beta)$. Eqs. (39) and (36) show that $\ln Z(N, \beta)/V$, to leading order for large V , increases monotonically with ρ till $\rho_c(\beta)$ (fluid phase) and then “freezes” to the value $\zeta(d+1)/\beta^d$ for $\rho > \rho_c(\beta)$ in the condensed phase (see Fig. 3).

Identifying $-\ln Z(N, \beta)/V$ for large V as the free energy per unit volume in the thermodynamic limit, denoted by

$$f(\rho, \beta) = -\lim_{V \rightarrow \infty} \frac{\ln Z(N, \beta)}{V}, \quad (40)$$

we now summarise how $f(\rho, \beta)$ behaves across the critical density $\rho_c(\beta) = \zeta(d)/\beta^d$. We find

$$-f(\rho, \beta) = \lim_{V \rightarrow \infty} \frac{\ln Z(N, \beta)}{V} = \begin{cases} \rho s^* + \frac{1}{\beta^d} \text{Li}_{d+1}(e^{-s^*}) & , \quad \rho < \rho_c(\beta) \text{ (fluid)} \\ \frac{\zeta(d+1)}{\beta^d} & , \quad \rho > \rho_c(\beta) \text{ (condensed)} , \end{cases} \quad (41)$$

where s^* , in the first line, is given by the solution of $\text{Li}_d(e^{-s^*}) = \rho \beta^d$. Thus the free energy per unit volume in the thermodynamic limit undergoes a *freezing* transition as the density ρ crosses from the fluid side to the condensed side.

Let us end this section with the following side remark. Whenever there is a saddle point in the integral in Eq. (25) at a finite value $s = s^*$, i.e., the system is in the fluid phase ($\rho < \rho_c(\beta)$), the canonical and the grand-canonical ensembles are equivalent. However, in the condensed phase for $\rho > \rho_c(\beta)$, there is no longer a saddle in $A(s, \rho)$ in Eq. (25) and, in that case, we have analysed the large N behavior of the canonical partition function by directly evaluating the Bromwich integral near $s = 0$. This is the correct procedure to follow to compute not just the leading order but also the subleading orders to the large V behavior of the partition function $Z(N, \beta)$. This is different from the standard procedure used in textbooks [20, 21] where one assumes that there is an “effective” grand canonical description even in the condensed side, with a new saddle point that occurs at $s^* \sim O(1/(V(\rho - \rho_c(\beta))))$. For instance, for the Bose gas in the harmonic trap this route was also recently used in Ref. [34]. There, the partition function in Eq. (25) was rewritten as

$$Z(N, \beta) = \int_{\Gamma} \frac{ds}{2\pi i} e^{V(A(s, \rho) - \frac{1}{V} \ln(1 - e^{-s}))} , \quad (42)$$

and a saddle point was sought for the new effective action modified by the presence of the order $O(1/V)$ correction term. Evaluating the action at the new saddle point provides correctly the leading order of the partition function. However, the subleading corrections are not correctly captured by this effective saddle point method. For that, one needs to perform carefully the Bromwich integral along the vertical axis close to $s = 0$, as is done here. A more concrete example of this is provided in the next subsection.

3.3 Connecting the fluid and the condensed phase on a smaller scale of $(\rho - \rho_c(\beta)) \sim O(1/\sqrt{V})$

In the previous two subsections, we have seen that, to leading order for large V , the free energy per unit volume undergoes a freezing transition at $\rho = \rho_c(\beta)$. More precisely, for small $(\rho - \rho_c(\beta))$, one has from Eqs. (36) and (41)

$$\begin{aligned} -f(\rho, \beta) &= \lim_{V \rightarrow \infty} \frac{\ln Z(N, \beta)}{V} \\ &= \begin{cases} \frac{\zeta(d+1)}{\beta^d} - \frac{\beta^d}{4\zeta(d-1)}(\rho_c(\beta) - \rho)^2 & , \quad \rho < \rho_c(\beta) \text{ (fluid)} \\ \frac{\zeta(d+1)}{\beta^d} & , \quad \rho > \rho_c(\beta) \text{ (condensed)} . \end{cases} \end{aligned} \quad (43)$$

Thus the second derivative of $f(\rho, \beta)$ with respect to ρ is discontinuous at $\rho = \rho_c(\beta)$. It is interesting to understand how, for large but finite V , the free energy per unit volume of the two phases get continuously connected. In other words, if we zoom out the region in the vicinity of $\rho = \rho_c(\beta)$ in Fig. 3 and appropriately scale $(\rho - \rho_c(\beta))$ with V , how do the left and right side of $\rho_c(\beta)$ in Fig. 3 match smoothly with each other?

To achieve this matching, we start with the expression for the partition function in Eq. (37), which is actually valid for both $\rho < \rho_c(\beta)$ and $\rho > \rho_c(\beta)$. Next we rescale $s\sqrt{V} = \tilde{s}$ to get

$$Z(N, \beta) \approx e^{V \frac{\zeta(d+1)}{\beta^d}} \int_{\Gamma} \frac{d\tilde{s}}{2\pi i} \frac{1}{\tilde{s}} e^{\sqrt{V}(\rho - \rho_c(\beta))\tilde{s} + \frac{\zeta(d-1)}{\beta^d}\tilde{s}^2 + \dots} . \quad (44)$$

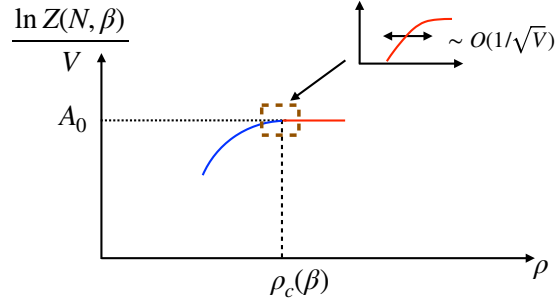


Figure 3: Plot of the $\ln Z(N, \beta)/V$ (in the limit $V \rightarrow \infty$) vs ρ close to the critical density $\rho = \rho_c(\beta)$ as given in Eq. (43). The curve decreases quadratically for $\rho < \rho_c(\beta)$ (shown by the blue line), and freezes to the constant $A_0 = \zeta(d+1)/\beta^d$ for $\rho > \rho_c(\beta)$ (as shown by the red horizontal line). In the inset, we zoom in in the region where $\rho - \rho_c(\beta) = O(1/\sqrt{V})$ and show schematically how the crossover occurs from the left (fluid) to the right (condensed), as obtained by taking the logarithm in Eq. (47).

We now consider the limit $\rho \rightarrow \rho_c(\beta)$ and $V \rightarrow \infty$ but with the product $\sqrt{V}(\rho - \rho_c(\beta)) = y$ fixed. In this limit, one can see that all the higher order terms denoted by \dots in (44) drop out of the integral, leading to

$$Z(N, \beta) \approx e^{V \frac{\zeta(d+1)}{\beta^d}} \int_{\Gamma} \frac{d\tilde{s}}{2\pi i} \frac{1}{\tilde{s}} e^{y\tilde{s} + \frac{\zeta(d-1)}{\beta^d} \tilde{s}^2}. \quad (45)$$

Taking a derivative with respect to y makes it a simple Gaussian integral and one gets

$$\frac{\partial}{\partial y} Z(N, \beta) \approx e^{V \frac{\zeta(d+1)}{\beta^d}} \frac{1}{\sqrt{4\pi b}} e^{-\frac{y^2}{4b}}, \quad b = \frac{\zeta(d-1)}{\beta^d}. \quad (46)$$

Integrating this back with respect to y and using the fact that $Z(N, \beta) \rightarrow 0$ as $y \rightarrow -\infty$ one gets

$$Z(N, \beta) \approx \frac{e^{V \frac{\zeta(d+1)}{\beta^d}}}{2} \left[1 + \operatorname{erf} \left(\frac{(\rho - \rho_c(\beta))\sqrt{V}}{\sqrt{4b}} \right) \right], \quad b = \frac{\zeta(d-1)}{\beta^d}, \quad (47)$$

where $\operatorname{erf}(x) = 2/\sqrt{\pi} \int_0^x e^{-u^2} du$ and we used $y = (\rho - \rho_c(\beta))\sqrt{V}$. Let us recall the asymptotic behaviours of the error function, namely

$$\operatorname{erf}(x) \approx 1 - \frac{e^{-x^2}}{|x|\sqrt{\pi}}, \quad x \rightarrow \pm\infty. \quad (48)$$

Therefore, when $(\rho - \rho_c(\beta)) > 0$ and $(\rho - \rho_c(\beta)) \gg 1/\sqrt{V}$ one gets from (47) and (48) for large positive x , one recovers the result in the condensed phase given in the second line of Eq. (43). In contrast, for $(\rho - \rho_c(\beta)) < 0$ and $(\rho_c(\beta) - \rho) \gg 1/\sqrt{V}$, one gets from (47) and (48) for large negative x the behavior in the fluid phase given in the first line of Eq. (43). Thus the result in Eq. (47) is the crossover function that smoothly connects the partition functions on both sides. Let us remark that, to compute this crossover function accurately, we needed to perform the Bromwich integral close to $s = 0$. If, instead, we had used the effective saddle point approach mentioned before, it would have given the leading order $e^{O(V)}$ term in Eq. (47) correctly, but not the crossover function which requires a more careful analysis of the Brownmitch integral, as done above.

Let us end this section by drawing a comparison to a similar condensation transition observed in interacting particle systems, such as the zero range process (ZRP) [35,36]. The ZRP is defined on a lattice where each site contains n_i particles and a single particle from site i can jump to its neighboring sites with a rate that depends only on n_i . The dynamics conserves the total number of particles. In this model, for a certain choice of the hopping rate, the system undergoes a condensation phase transition when the density ρ of particles exceeds a critical value. In the condensed phase, one single site carries a macroscopic fraction of particles. Thus, unlike in the Bose gas case studied here, where the condensation occurs in the momentum/energy space, in ZRP and related models the condensation occurs in the real space [37, 38]. In the low density fluid phase, the grand canonical partition function can again be evaluated by the saddle point method and in this case the canonical and the grand-canonical ensembles are equivalent. However, in the condensed phase, the saddle hits the origin and, to evaluate the canonical partition function, one can no longer use the equivalence to the grand-canonical ensemble [37, 38]. Instead, one has to evaluate the canonical partition by performing the Bromwich integral close to $s = 0$ [37, 38], as in the Bose gas case studied here. Similar real space condensation scenarios appeared recently in a number of contexts: this includes, e.g., the distribution of the position of a run-and-tumble particle in d -dimensions [39–41] and the localization/delocalization transition in discrete nonlinear Schrödinger equation [42,43]. However, there is an important difference in details between such real space condensation models like the ZRP and the noninteracting trapped Bose gas considered here. In the ZRP case, the canonical partition function can be expressed in a similar way as in Eq. (25) for the Bose gas, with the important difference that the corresponding action $A(s, \rho)$ vanishes at $s = 0$ in the ZRP [38], while it is non zero in the Bose gas case. Hence in ZRP the subleading corrections in the small s expansion of $A(s, \rho)$ in (25) are important. In particular, it turns out that the singular terms in the expansion in Eqs. (32) and (33) play an important role in ZRP to determine the partition function in the thermodynamic limit [38]. However, in the Bose gas studied here, such singular terms in the small s expansion only contribute to sub-leading order, since $A(0, \rho) \neq 0$ in Eq. (25).

4 Statistics of the moment of inertia

In this section we study the statistics of $I = \omega^2 \sum_i \vec{r}_i^2$ at finite temperature T , where we have set $m = 1$ in Eq. (6). Having obtained the partition function $Z(N, \beta)$ in the large N limit in the previous section, we will now use these results in the exact relation in Eq. (17) to compute the statistics of I .

We first start with the average $\langle I \rangle = -\partial_\beta \ln Z(N, \beta)$ given in Eq. (20). In the fluid phase where $\rho < \rho_c(\beta)$, by using the expression of $\ln Z(N, \beta)/V$ in Eqs. (35) and (36), and taking derivative w.r.t. β , one can in principle implicitly compute this average for all $\rho < \rho_c(\beta)$. However, it is easier to work with the expansion of $\ln Z(N, \beta)/V$ close to $\rho = \rho_c(\beta)$ in either phases, as given in Eq. (43). Taking a derivative of that expression in (43) w.r.t β one gets, up to leading order in $(\rho - \rho_c(\beta))$

$$\frac{\langle I \rangle}{V} \underset{V \rightarrow \infty}{=} \begin{cases} \frac{d\zeta(d+1)}{\beta^{d+1}} - \frac{d\zeta(d)}{2\zeta(d-1)\beta}(\rho_c(\beta) - \rho) + \frac{d\beta^{d-1}}{4\zeta(d-1)}(\rho_c(\beta) - \rho)^2 & , \quad \rho < \rho_c(\beta) , \\ \frac{d\zeta(d+1)}{\beta^{d+1}} & , \quad \rho > \rho_c(\beta) . \end{cases} \quad (49)$$

Thus while the average $\langle I \rangle/V$ is itself is continuous at $\rho = \rho_c(\beta)$, its first derivative w.r.t ρ is discontinuous at $\rho = \rho_c(\beta)$. This is our first real space diagnostic of the BEC transition.

Let us now turn to the variance. Our starting point is the exact relation in Eq. (21), which holds for all ω . However, since we will work in the appropriate thermodynamic limit where $\omega \rightarrow 0$ and $N \rightarrow \infty$ with $N \omega^d = \rho$ fixed, we first take the $\omega \rightarrow 0$ limit in Eq. (21) which then reads

$$\text{Var}(I) = \langle I^2 \rangle - \langle I \rangle^2 \underset{\omega \rightarrow 0}{=} \left[\frac{\partial^2 \ln Z}{\partial \beta^2} + \frac{1}{\beta} \langle I \rangle \right]. \quad (50)$$

We now take two derivatives w.r.t. β in Eq. (43) and also use the expression of $\langle I \rangle$ in Eq. (49). After a long but straightforward algebra we get

$$\frac{\text{Var}(I)}{V} \underset{V \rightarrow \infty}{=} \begin{cases} \frac{1}{\beta^{d+2}} \left[d(d+2)\zeta(d+1) - \frac{d^2\zeta^2(d)}{2\zeta(d-1)} \right] + \frac{2(d-2)\zeta(d)}{2\beta^2\zeta(d-1)} (\rho_c(\beta) - \rho) \\ \quad + \beta^{d-2} \frac{d(2-d)}{4\zeta(d-1)} (\rho_c(\beta) - \rho)^2 & , \quad \text{for } \rho < \rho_c(\beta) , \\ \frac{d(d+2)\zeta(d+1)}{\beta^{d+2}} & , \quad \text{for } \rho > \rho_c(\beta) . \end{cases} \quad (51)$$

Thus, as ρ approaches $\rho_c(\beta)$ from above and below, the variance of I is discontinuous across $\rho = \rho_c(\beta)$. This discontinuity provides another real space signature of the BEC transition.

Having obtained the nonanalytic behaviors of both the mean and the variance at the critical density $\rho = \rho_c(\beta)$, it is natural to wonder how the full distribution of I behave as one changes the density ρ . We will now show that the distribution $P_\beta(I, N)$ in Eq. (15) admits a large deviation principle in the thermodynamic limit (when $\omega \rightarrow 0$, or equivalently $V = \omega^{-d} \rightarrow \infty$ and also $N \rightarrow \infty$ but with the density $\rho = N/V$ kept fixed). This large deviation behavior can be expressed as

$$P_\beta(I, N) \approx e^{-V \Phi(\frac{I}{V})}, \quad (52)$$

where we will see that the rate function $\Phi(z)$ has two distinct behaviors respectively in the fluid phase ($\rho < \rho_c(\beta)$) and in the condensed phase ($\rho > \rho_c(\beta)$). Upon substituting this anticipated form (52) in the Laplace transform $\tilde{P}_\beta(\lambda, N)$ in Eq. (16) gives

$$\tilde{P}_\beta(\lambda, N) = \langle e^{-\lambda I} \rangle \approx \int_0^\infty e^{-\lambda I - V \Phi(\frac{I}{V})} dI. \quad (53)$$

Performing the change of variable $I/V = z$ and evaluating the resulting integral over z by a saddle point method, assuming it exists, one gets

$$\tilde{P}_\beta(\lambda, N) \approx e^{-V \Psi(\lambda)} \quad , \quad \text{with} \quad \Psi(\lambda) = \min_z [\lambda z + \Phi(z)]. \quad (54)$$

Taking logarithm on both sides, we see that

$$\Psi(\lambda) \approx -\frac{1}{V} \ln \langle e^{-\lambda I} \rangle \quad (55)$$

is nothing but the cumulant generating function of the random variable I . By inverting the Legendre transform in Eq. (54), one can express $\Phi(z)$ in terms of $\Psi(\lambda)$ via the relation

$$\Phi(z) = \max_\lambda [-\lambda z + \Psi(\lambda)]. \quad (56)$$

Thus, to derive $\Phi(z)$, we need to determine $\Psi(\lambda)$ and then Eq. (56) gives access to $\Phi(z)$.

4.1 Computation of $\Psi(\lambda)$

To determine $\Psi(\lambda)$, we can now make use of the exact relation in Eq. (17) and the already derived large V behaviour of the partition function $Z(N, \beta)$ in the previous section. To use this relation (17), we need to first determine $\tilde{\beta}(\lambda)$ as a function of β and λ using Eq. (18). Taking the $\omega \rightarrow 0$ limit (since we are working in the thermodynamic limit) gives simply

$$\tilde{\beta} = \sqrt{\beta(\beta + 2\lambda)} . \quad (57)$$

For $\tilde{\beta}$ to be real, we need the hard constraint $\lambda \geq -\beta/2$. This simply means that the Laplace transform $\langle e^{-\lambda I} \rangle$ in Eq. (52) diverges as $\lambda \rightarrow -\beta/2$ indicating that $\lambda \in [-\beta/2, +\infty)$ is the allowed range of the real part of λ . Using this relation in Eq. (18) and (54) then gives, in the thermodynamic limit,

$$\tilde{P}_\beta(\lambda, N) = \langle e^{-\lambda I} \rangle \approx e^{-V\Psi(\lambda)} \approx \frac{Z(N, \sqrt{\beta(\beta + 2\lambda)})}{Z(N, \beta)} . \quad (58)$$

Taking logarithm on both sides then gives the desired rate function $\Psi(\lambda)$ in terms of the partition function $Z(N, \beta)$

$$\Psi(\lambda) = \lim_{V \rightarrow \infty} \left[-\frac{1}{V} \ln Z \left(N, \sqrt{\beta(\beta + 2\lambda)} \right) + \frac{1}{V} \ln Z(N, \beta) \right] . \quad (59)$$

Therefore $\Psi(\lambda)$ has a nice physical interpretation. Recalling the definition of the free energy per unit volume in Eq. (40), we see that $\Psi(\lambda)$ represents the free energy difference between two “species” of ideal Bose gases: one (A) which is held at inverse temperature β and the second (B) which is held at inverse temperature $\tilde{\beta} = \sqrt{\beta(\beta + 2\lambda)}$ given in Eq. (57). Thus Eq. (59) reads

$$\Psi(\lambda) = f_B \left(\rho, \sqrt{\beta(\beta + 2\lambda)} \right) - f_A(\rho, \beta) , \quad (60)$$

For the species A, the critical density that separates its fluid phase from its condensed counterpart is $\rho_c(\beta)$ given in Eq. (30), which of course is independent of λ . For species B, on the other hand, the corresponding critical density is given by $\rho_c(\tilde{\beta})$ where $\tilde{\beta}$ is given in (57) and clearly it depends on λ . The critical densities for the two species are given explicitly by

$$\rho_c(\beta) = \frac{\zeta(d)}{\beta^d} , \quad \rho_c(\tilde{\beta}) = \frac{\zeta(d)}{\tilde{\beta}^d} = \frac{\zeta(d)}{[\beta(\beta + 2\lambda)]^{d/2}} . \quad (61)$$

Thus, for a fixed inverse temperature β , the function $\Psi(\lambda)$ exhibits different behaviors in the (λ, ρ) plane. We recall that the allowed range of λ is $\lambda \in [-\beta/2, +\infty)$ and ρ can be any positive number. This allowed range in the (λ, ρ) plane is shown in Fig. 4. In this figure, the horizontal black line denotes $\rho_c(\beta)$ for the species A given in (61) which, as mentioned before, is independent of λ . The dark blue line denotes the other critical density $\rho_c(\tilde{\beta})$ in (61) for the species B. These two critical lines divide the allowed region in (λ, ρ) plane into four distinct phases (see Fig. 4):

- (i) The fluid-fluid (F-F) phase where $\rho < \rho_c(\beta)$ and $\rho < \rho_c(\tilde{\beta})$. In this phase, both species A and B are in their respective fluid phases.
- (ii) The fluid-condensed (F-C) phase where $\rho < \rho_c(\beta)$ but $\rho > \rho_c(\tilde{\beta})$. Here, the species A is still in its fluid phase but species B is in its condensed phase.

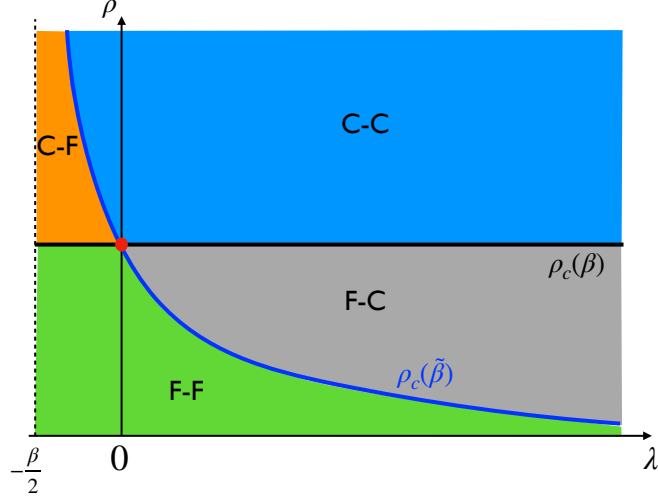


Figure 4: Phase diagram in the (λ, ρ) plane. The allowed values of λ lie in the range $\lambda \in (-\beta/2, +\infty)$ and $\rho \geq 0$. The black horizontal line represents the physical critical density $\rho = \rho_c(\beta)$, which is independent of λ . The solid blue curve represents $\rho_c(\tilde{\beta})$ with $\tilde{\beta} = \sqrt{\beta(\beta + 2\lambda)}$, as given in Eq. (61) and it diverges as $\lambda \rightarrow -\beta/2$. These two curves meet at $(\lambda = 0, \rho = \rho_c(\beta))$, marked by a red filled circle. The four colored phases representing the fluid-fluid (F-F), the fluid-condensed (F-C), the condensed-fluid (C-F) and the condensed-condensed (C-C) meet at the red filled circle.

- (iii) The condensed-fluid (C-F) phase where $\rho > \rho_c(\beta)$, while $\rho < \rho_c(\tilde{\beta})$. In this case, the species A is in the condensed phase, while the species B is in the fluid phase.
- (iv) The condensed-condensed (C-C) phase where $\rho > \rho_c(\beta)$ and $\rho > \rho_c(\tilde{\beta})$. Here both species are in their condensed phases.

Since the partition function for each species behaves differently across its critical density, the free energy per unite volume $f_A(\rho, \beta)$ and $f_B(\rho, \beta)$ will also behave differently across the critical densities for each species. Hence, $\Psi(\lambda)$ in Eq. (60) will also behave differently in each of the four different phases in the (λ, ρ) plane in Fig. 4. These different behaviors are derived below. For convenience, we will denote the free energies per unit volume for each species A and B, respectively in the fluid and the condensed phases as $f_{A,B}^F(\rho, \beta)$ and $f_{A,B}^C(\rho, \beta)$, where the superscripts F and C refer to the fluid and the condensed phases.

4.1.1 The F-F phase

In this phase both species are in their respective fluid phases, since $\rho < \rho_c(\beta)$ and $\rho < \rho_c(\tilde{\beta})$. Hence, in this case, we have

$$\Psi(\lambda) = f_B^F(\rho, \beta) - f_A^F(\rho, \beta) . \quad (62)$$

We can then use the expression given in Eq. (35) for both species. This leads to

$$\Psi(\lambda) = -\rho\tilde{s}^* - \frac{1}{\tilde{\beta}^d} \text{Li}_{d+1}(e^{-\tilde{s}^*}) + \rho s^* + \frac{1}{\beta^d} \text{Li}_{d+1}(e^{-s^*}) \quad (63)$$

where s^* and \tilde{s}^* denote respectively the saddle points for species A and B and are given implicitly as the solutions of

$$\text{Li}_d(e^{-s^*}) = \rho \beta^d \quad , \quad \text{and} \quad \text{Li}_d(e^{-\tilde{s}^*}) = \rho \tilde{\beta}^d = \rho [\beta(\beta + 2\lambda)]^{d/2} . \quad (64)$$

We compute $\Psi(\lambda)$ for a fixed ρ in the F-F phase by varying λ . For a given ρ in this phase, we note that the condition $\rho < \rho_c(\tilde{\beta})$ indicates that $\lambda < \lambda_c$ where

$$\lambda_c = \frac{1}{2} \left(\frac{1}{\tilde{\beta}} \left[\frac{\zeta(d)}{\rho} \right]^{2/d} - \beta \right). \quad (65)$$

Therefore in this phase, the allowed range of λ is $-\beta/2 < \lambda < \lambda_c$. In principle, for a given ρ and λ in the F-F phase, one can obtain s^* and \tilde{s}^* numerically from Eq. (64) and, hence, determine $\Psi(\lambda)$ numerically from Eq. (63). A plot of this $\Psi(\lambda)$ is given in Fig. 5. However, one can extract analytically the asymptotic behavior of $\Psi(\lambda)$ as $\lambda \rightarrow -\beta/2$ as well as $\lambda \rightarrow \lambda_c$.

The limit $\lambda \rightarrow -\beta/2$. In this case $\tilde{\beta} \rightarrow 0$ from Eq. (57). From Eq. (64), together with the asymptotic expansion given in Eq. (28), it follows that, to leading order, $e^{-\tilde{s}^*} \approx \rho \tilde{\beta}^d$. Consequently,

$$\tilde{s}^* \rightarrow -\frac{d}{2} \ln(\beta + 2\lambda) \quad , \quad \text{as } \lambda \rightarrow -\beta/2. \quad (66)$$

Substituting this behavior back in Eq. (63) one finds, to leading order

$$\Psi(\lambda) \approx \rho \frac{d}{2} \ln(\beta + 2\lambda) + c_0 \quad , \quad \text{as } \lambda \rightarrow -\beta/2, \quad (67)$$

where c_0 is an unimportant constant independent of λ .

The limit $\lambda \rightarrow \lambda_c$. In this limit, the species B is close to its critical density $\rho_c(\tilde{\beta})$. Hence we can use the saddle point approximation of the free energy given in the first line of Eq. (43), after replacing β by $\tilde{\beta}$. This gives

$$f_B^F(\rho, \beta) = \frac{\zeta(d+1)}{[\tilde{\beta}(\lambda)]^d} - \frac{[\tilde{\beta}(\lambda)]^d}{4\zeta(d-1)} \left(\frac{\zeta(d)}{[\tilde{\beta}(\lambda)]^d} - \rho \right)^2, \quad (68)$$

where we used $\rho_c(\tilde{\beta}) = \zeta(d)/[\tilde{\beta}(\lambda)]^d$ and we recall that $\tilde{\beta}(\lambda) = \sqrt{\beta(\beta + 2\lambda)}$. We now need to expand $f_B^F(\rho, \beta)$ in Eq. (68) for λ close to λ_c where λ_c is given in Eq. (65). We set $\lambda = \lambda_c - \epsilon$ in the expression for $\tilde{\beta}(\lambda)$ in Eq. (57). We also notice from Eq. (65) that

$$[\beta(\beta + 2\lambda_c)]^{d/2} = \frac{\zeta(d)}{\rho}. \quad (69)$$

By expanding up to order $O(\epsilon^2)$ we then get

$$[\tilde{\beta}(\lambda)]^d = \frac{\zeta(d)}{\rho} \left[1 - \frac{d}{(\beta + 2\lambda_c)} \epsilon + \frac{d(d-2)}{2(\beta + 2\lambda_c)^2} \epsilon^2 + O(\epsilon^3) \right]. \quad (70)$$

Substituting this expansion in the expression of $f_B^F(\rho, \beta)$ in Eq. (68) we get

$$f_B^F(\rho, \beta) = -\frac{\rho \zeta(d+1)}{\zeta(d)} - \frac{d \zeta(d+1)}{\zeta(d)} \frac{\rho}{\beta + 2\lambda_c} \epsilon - A_2 \epsilon^2 + O(\epsilon^3), \quad (71)$$

where

$$A_2 = \frac{d \rho \left(-d[\zeta(d)]^2 + 2(d+2)\zeta(d-1)\zeta(d+1) \right)}{4\zeta(d)\zeta(d-1)(\beta + 2\lambda_c)^2}. \quad (72)$$

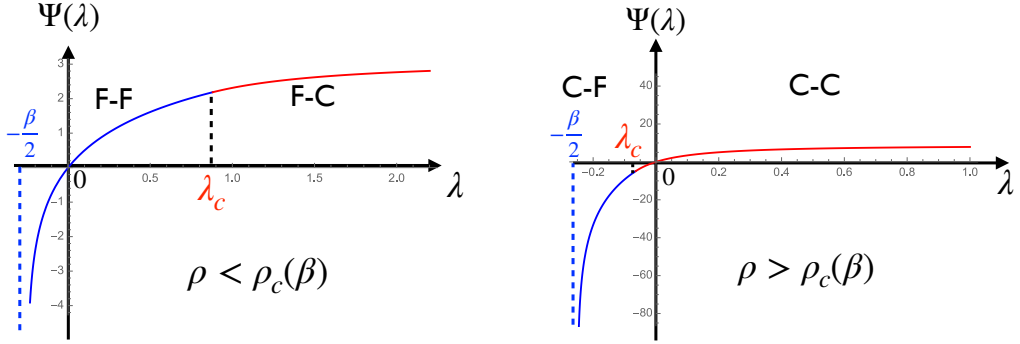


Figure 5: The function $\Psi(\lambda)$ plotted as a function of λ for $\rho < \rho_c(\beta)$ (left panel) and $\rho > \rho_c(\beta)$ (right panel). In both panels, λ_c marks the value of λ that separates two phases as one increases λ and the value of λ_c is given in Eq. (65). In the figure, we used $\beta = 1/2$. On the left panel, λ_c separates the F-F and the F-C phases, while on the right panel it separates the C-F and the C-C phases. As λ crosses λ_c , in both panels, the functions $\Psi(\lambda)$ and its first derivative are continuous, while the second derivative $\Psi''(\lambda)$ undergoes a discontinuous jump (though not visible in the figure).

One can check that $A_2 > 0$.

On the other hand, for the species A, its free energy is independent of λ and corresponds to its fluid phase and hence is given by $f_A^F(\rho, \beta)$. Therefore $\Psi(\lambda)$ in Eq. (60), close to λ_c in the F-F phase behaves as

$$\Psi(\lambda) = -f_A^F(\rho, \beta) - \frac{\rho \zeta(d+1)}{\zeta(d)} - \frac{d \zeta(d+1)}{\zeta(d)} \frac{\rho}{\beta + 2\lambda_c} (\lambda_c - \lambda) - A_2 (\lambda_c - \lambda)^2 + O((\lambda_c - \lambda)^3). \quad (73)$$

We will see later that the second derivative of $\Psi(\lambda)$, i.e., the amplitude of $(\lambda_c - \lambda)^2$ in this expansion, undergoes a discontinuous jump when λ_c is approached from above, i.e., from the F-C side in Fig. 4.

4.1.2 The F-C phase

Now we consider the F-C phase with $\rho < \rho_c(\beta)$ and $\rho > \rho_c(\tilde{\beta})$. This corresponds to the grey shaded area in Fig. 4. We fix ρ and vary λ . Clearly in this regime λ varies from λ_c to $+\infty$. We want to calculate $\Psi(\lambda)$ in this phase, for $\lambda \in [\lambda_c, +\infty)$. Noting that, for the species B, the system is in the condensed phase, the free energy $f_B^F(\rho, \beta)$ has a simple expression given in the second line of Eq. (41). Consequently, for any $\lambda \in [\lambda_c, +\infty)$, we get

$$\Psi(\lambda) = f_B^C(\rho, \beta) - f_A^F(\rho, \beta) = -f_A^F(\rho, \beta) - \frac{\zeta(d+1)}{[\tilde{\beta}(\lambda)]^d} = -f_A^F(\rho, \beta) - \frac{\zeta(d+1)}{[\beta(\beta + 2\lambda)]^{d/2}}. \quad (74)$$

We recall that $f_A^F(\rho, \beta)$ is independent of λ . Below, we will compute the asymptotic behaviors of $\Psi(\lambda)$ in the two opposite limits $\lambda \rightarrow \infty$ and $\lambda \rightarrow \lambda_c$ (from above, i.e., $\lambda > \lambda_c$).

The limit $\lambda \rightarrow +\infty$. In this limit, it follows trivially from Eq. (74) that

$$\Psi(\lambda) \approx -f_A^F(\rho, \beta) - \frac{\zeta(d+1)}{(2\beta \lambda)^{d/2}}, \quad \text{as } \lambda \rightarrow +\infty. \quad (75)$$

The limit $\lambda \rightarrow \lambda_c$. In this limit, substituting the expansion of $[\tilde{\beta}(\lambda)]^d$ from Eq. (70) in Eq. (74), we get

$$\Psi(\lambda) = -f_A^F(\rho, \beta) - \frac{\rho \zeta(d+1)}{\zeta(d)} - \frac{d \zeta(d+1)}{\zeta(d)} \frac{\rho}{\beta + 2\lambda_c} (\lambda_c - \lambda) - A'_2 (\lambda_c - \lambda)^2 + O((\lambda_c - \lambda)^3), \quad (76)$$

where

$$A'_2 = \frac{d(d+2)\rho\zeta(d+1)}{2\zeta(d)(\beta + 2\lambda_c)^2}. \quad (77)$$

Summarising the behavior of $\Psi(\lambda)$ on both sides close to λ_c from Eqs. (73) and (76), we find

$$\Psi(\lambda) \approx \begin{cases} -f_A^F(\rho, \beta) - \frac{\rho \zeta(d+1)}{\zeta(d)} - \frac{d \zeta(d+1)}{\zeta(d)} \frac{\rho}{\beta + 2\lambda_c} (\lambda_c - \lambda) - A_2 (\lambda_c - \lambda)^2, & \lambda \rightarrow \lambda_c^- \\ -f_A^F(\rho, \beta) - \frac{\rho \zeta(d+1)}{\zeta(d)} - \frac{d \zeta(d+1)}{\zeta(d)} \frac{\rho}{\beta + 2\lambda_c} (\lambda_c - \lambda) - A'_2 (\lambda_c - \lambda)^2, & \lambda \rightarrow \lambda_c^+, \end{cases} \quad (78)$$

Thus, comparing the expansions of $\Psi(\lambda)$ from above and below λ_c , we see that, while $\Psi(\lambda)$ and its first derivative $\Psi'(\lambda)$ are both continuous at $\lambda = \lambda_c$, the second derivative undergoes a discontinuous jump given by

$$\Psi''(\lambda_c^+) - \Psi''(\lambda_c^-) = 2(A_2 - A'_2) = -\frac{\rho d^2 \zeta(d)}{2\zeta(d-1)(\beta + 2\lambda_c)^2} = -\frac{\beta^2 d^2 \rho^{\frac{4}{d}+1}}{2[\zeta(d)]^{\frac{4}{d}-1}}. \quad (79)$$

4.1.3 The C-F and the C-C phases

The C-F phase corresponds to $\rho > \rho_c(\beta)$ and $\rho < \rho_c(\tilde{\beta})$, while the C-C phase corresponds to $\rho > \rho_c(\beta)$ and $\rho > \rho_c(\tilde{\beta})$. Thus, fixing $\rho > \rho_c(\beta)$, as we vary λ , the C-F phase corresponds to the region $\lambda \in (-\beta/2, \lambda_c]$ (shown by the orange shade in Fig. 4) and the C-C phase corresponds to $\lambda \in [\lambda_c, +\infty)$ (shown by the blue shade in Fig. 4). Here λ_c is given by the same expression as in Eq. (65). As λ increases through λ_c , for fixed $\rho > \rho_c(\beta)$, the behaviour of $\Psi(\lambda)$ is rather similar to the analysis presented in the previous subsection for $\rho < \rho_c(\beta)$. The only difference is that the free energy per unit volume of the species A is now given by $f_A^C(\rho, \beta)$. More precisely $\Psi(\lambda)$ is given by

$$\Psi(\lambda) = \begin{cases} -f_A^C(\rho, \beta) + f_B^F(\rho, \beta) & , \quad (\text{C-F phase}), \\ -f_A^C(\rho, \beta) + f_B^C(\rho, \beta) & , \quad (\text{C-C phase}). \end{cases} \quad (80)$$

For the contribution $f_B^F(\rho, \beta)$ and $f_B^C(\rho, \beta)$ from the species B, one gets exactly the same expressions as in Eq. (41), with β replaced by $\tilde{\beta}$. Skipping further details, let us summarise the main limiting behaviors of $\Psi(\lambda)$ as λ varies from $-\beta/2$ to $+\infty$.

The limit $\lambda \rightarrow -\beta/2$. In this case

$$\Psi(\lambda) \approx \rho \frac{d}{2} \ln(\beta + 2\lambda) + c'_0 \quad , \quad \text{as} \quad \lambda \rightarrow -\beta/2, \quad (81)$$

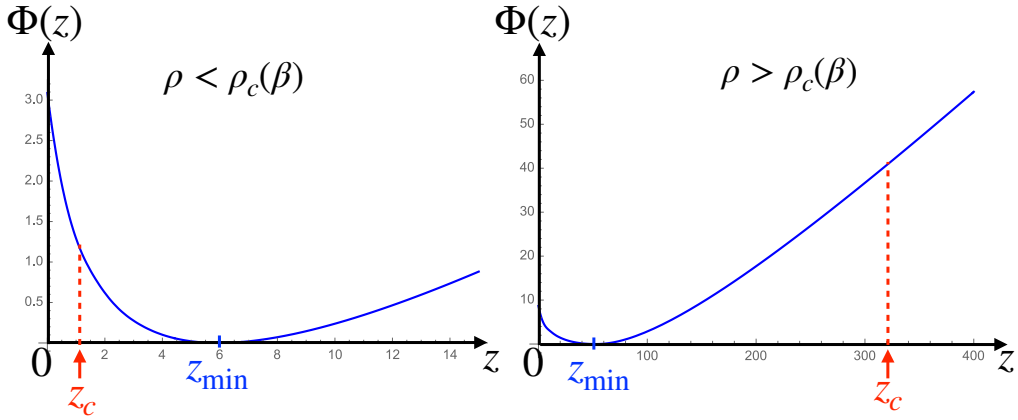


Figure 6: Plot of the rate function $\Phi(z)$ vs z for $\rho < \rho_c(\beta)$ (left panel) and $\rho > \rho_c(\beta)$ (right panel), which has been obtained by evaluating numerically the Legendre transform of $\Psi(\lambda)$ in Eq. (85). In both panels, the function $\Phi(z)$ vanishes at z_{\min} quadratically as in Eq. (94). The rate function $\Phi(z)$ has a singularity at $z = z_c$, given in Eq. (96). At $z = z_c$, while the functions $\Phi(z)$ and its first derivative are continuous, its second derivative undergoes a discontinuous jump as given in (97). On the left panel where $\rho < \rho_c(\beta)$ (fluid phase), the singular point z_c is to the left of z_{\min} , while on the right panel (condensed phase), z_c is on the right side of z_{\min} . Here we used $\beta = 1/2$.

where c'_0 is an unimportant constant independent of λ and is different from c_0 in Eq. (67).

The limit $\lambda \rightarrow \lambda_c$. In this case, up to quadratic order in $(\lambda_c - \lambda)$ one gets

$$\Psi(\lambda) \approx \begin{cases} -f_A^C(\rho, \beta) - \frac{\rho \zeta(d+1)}{\zeta(d)} - \frac{d \zeta(d+1)}{\zeta(d)} \frac{\rho}{\beta + 2\lambda_c} (\lambda_c - \lambda) - A_2 (\lambda_c - \lambda)^2, & \lambda \rightarrow \lambda_c^- \\ -f_A^C(\rho, \beta) - \frac{\rho \zeta(d+1)}{\zeta(d)} - \frac{d \zeta(d+1)}{\zeta(d)} \frac{\rho}{\beta + 2\lambda_c} (\lambda_c - \lambda) - A'_2 (\lambda_c - \lambda)^2, & \lambda \rightarrow \lambda_c^+, \end{cases} \quad (82)$$

where the constants A_2 and A'_2 are exactly the same as in Eqs. (72) and (77) respectively. Thus, as in the case $\rho < \rho_c(\beta)$, the second derivative $\Psi''(\lambda)$ undergoes exactly the same discontinuous jump given in Eq. (79).

The limit $\lambda \rightarrow +\infty$. In this case, the expression for $\Psi(\lambda)$ is given by

$$\Psi(\lambda) = f_B^C(\rho, \beta) - f_A^C(\rho, \beta) = -f_A^C(\rho, \beta) - \frac{\zeta(d+1)}{[\tilde{\beta}(\lambda)]^d} = -f_A^C(\rho, \beta) - \frac{\zeta(d+1)}{[\beta(\beta + 2\lambda)]^{d/2}}. \quad (83)$$

Hence, for large λ , one gets

$$\Psi(\lambda) \approx -f_A^C(\rho, \beta) - \frac{\zeta(d+1)}{(2\beta \lambda)^{d/2}}, \quad \text{as } \lambda \rightarrow +\infty. \quad (84)$$

4.2 Computation of the rate function $\Phi(z)$

We recall that the distribution of the moment of inertia I is given by the large deviation form in (52), where the rate function $\Phi(z)$ is related to $\Psi(\lambda)$ via the Legendre transform

$$\Phi(z) = \max_{\lambda} [-\lambda z + \Psi(\lambda)]. \quad (85)$$

In the previous section we have derived the behaviours of $\Psi(\lambda)$, as a function of λ , for fixed ρ and β . In this section, we will use these expressions for $\Psi(\lambda)$ in Eq. (85) to determine the rate function $\Phi(z)$. One can in principle determine numerically $\Phi(z)$ for all z from the known expression of $\Psi(\lambda)$. However, it is possible to extract analytically the asymptotic behaviors of $\Phi(z)$ in different limits, as shown below.

4.2.1 The limit $z \rightarrow \infty$

It turns out (and checked a posteriori) that, to determine the behaviour of $\Phi(z)$ as $z \rightarrow \infty$, we need to use the behavior of $\Psi(\lambda)$ as λ approaches its lowest allowed value $\lambda \rightarrow -\beta/2$. Indeed, substituting the leading behaviour of $\Psi(\lambda)$ from Eqs. (67) and (81) as $\lambda \rightarrow -\beta/2$ in Eq. (85), we get

$$\Phi(z) \approx \max_{\lambda} \left[-\lambda z + \rho \frac{d}{2} \ln(\beta + 2\lambda) \right], \quad (86)$$

where we have dropped the constant terms c_0 and c'_0 as they lead only to subleading corrections. The function $S(\lambda) = -\lambda z + \rho \frac{d}{2} \ln(\beta + 2\lambda)$ has a maximum at λ_{\max} given by

$$\beta + 2\lambda_{\max} = \frac{\rho d}{z}. \quad (87)$$

We see here, a posteriori, that a small value of $\beta + 2\lambda_{\max}$ indeed corresponds to large values of z . Substituting this λ_{\max} in (86) gives

$$\Phi(z) = S(\lambda_{\max}) \approx \frac{\beta}{2} z - \frac{\rho d}{2} \ln z + O(1) \quad , \quad \text{as } z \rightarrow \infty. \quad (88)$$

4.2.2 The limit $z \rightarrow 0$

In this limit, it turns out that we need to analyse the large λ behavior of $\Psi(\lambda)$. Substituting the large λ behaviours from Eqs. (75) and (84) in (85) we get

$$\Phi(z) = C + \max_{\lambda} \left[-\lambda z - \frac{\zeta(d+1)}{(2\beta\lambda)^{d/2}} \right], \quad (89)$$

where the constant C (independent of z) is given by $C = -f_A^F(\rho, \beta)$ (for $\rho < \rho_c(\beta)$) and by $C = -f_A^C(\rho, \beta)$ (for $\rho > \rho_c(\beta)$). Performing this maximisation w.r.t. λ , it turns out that $\lambda_{\max} = A_0 z^{-2/(d+2)}$ which clearly shows that z must be small in order that λ_{\max} is large, justifying a posteriori the use of the large λ expansion of $\Psi(\lambda)$ in Eq. (89). The constant A_0 is given by

$$A_0 = \left(\frac{d}{2} \frac{\zeta(d+1)}{(2\beta)^{d/2}} \right)^{2/(d+2)}. \quad (90)$$

Using this λ_{\max} in (89) gives, for small z ,

$$\Phi(z) \approx C - B_0 z^{\frac{d}{d+2}} \quad , \quad \text{as } z \rightarrow 0 \quad (91)$$

where the constant B_0 is simply related to A_0 .

4.2.3 The limit $z \rightarrow z_{\min}$

We now consider the behavior of $\Phi(z)$ close to $z = z_{\min}$ where z_{\min} denotes the value of z at which $\Phi(z)$ has a global minimum. We will see that this amounts to analysing $\Psi(\lambda)$ close to $\lambda = 0$. From Eq. (55), we see that the cumulant generating function $\Psi(\lambda)$ can always be expanded in a smooth power series of λ for small λ

$$\Psi(\lambda) = \frac{\langle I \rangle}{V} \lambda - \frac{\text{Var}(I)}{2V} \lambda^2 + O(\lambda^3). \quad (92)$$

Thus, substituting this expansion up to the quadratic order in Eq. (85), we get

$$\Phi(z) = \max_{\lambda} \left[- \left(z - \frac{\langle I \rangle}{V} \right) \lambda - \frac{1}{V} \text{Var}(I) \lambda^2 \right]. \quad (93)$$

Maximising w.r.t. λ , one obtains quite generically a quadratic form for $\Phi(z)$ close to $z = z_{\min} = \langle I \rangle / V$ given by

$$\Phi(z) \approx \frac{(z - z_{\min})^2}{2\sigma^2} \quad , \quad \text{where} \quad z_{\min} = \frac{\langle I \rangle}{V} \quad \text{and} \quad \sigma^2 = \frac{\text{Var}(I)}{V}. \quad (94)$$

Note that z_{\min} and σ^2 , in the $V \rightarrow \infty$ limit, can in principle be computed for any (ρ, β) from the partition function via Eqs. (20) and (50). In general, they have quite complicated expressions but, near $\rho = \rho_c(\beta)$, one can compute them explicitly as given in Eqs. (49) and (51).

4.2.4 The limit $z \rightarrow z_c$

It turns out that there is a “critical” point $z = z_c$ where the rate function $\Phi(z)$ and its derivative $\Phi'(z)$ are continuous, but the second derivative $\Phi''(z)$ is discontinuous. We will see that this actually corresponds to the singularity of $\Psi(\lambda)$ at $\lambda = \lambda_c$ found before. Indeed, substituting the expansions of $\Psi(\lambda)$ near $\lambda = \lambda_c$ from Eqs. (78) and (82), respectively for $\rho < \rho_c(\beta)$ and $\rho > \rho_c(\beta)$ in (85), and upon maximising w.r.t. λ we find the following results. For $\rho < \rho_c(\beta)$, we get

$$\Phi(z) \approx \begin{cases} f_A^F(\rho, \beta) - \frac{\rho \zeta(d+1)}{\zeta(d)} - \lambda_c z_c - \lambda_c(z - z_c) + \frac{(z - z_c)^2}{4A_2} & , \quad z > z_c \\ f_A^F(\rho, \beta) - \frac{\rho \zeta(d+1)}{\zeta(d)} - \lambda_c z_c - \lambda_c(z - z_c) + \frac{(z - z_c)^2}{4A'_2} & , \quad z < z_c , \end{cases} \quad (95)$$

where z_c is given by

$$z_c = \Psi'(\lambda_c) = \beta d \zeta(d+1) \left(\frac{\rho}{\zeta(d)} \right)^{\frac{d+2}{d}}. \quad (96)$$

For $\rho > \rho_c(\beta)$, exactly the same behavior occurs, except that $f_A^F(\rho, \beta)$ in both lines of (95) gets replaced by $f_C^F(\rho, \beta)$. From this expression (95) we see that, while $\Phi(z)$ and $\Phi'(z)$ are continuous at $z = z_c$, the second derivative $\Phi''(z)$ undergoes a discontinuous jump given by

$$\Phi''(z_c^+) - \Phi''(z_c^-) = \frac{1}{2} \left(\frac{1}{A_2} - \frac{1}{A'_2} \right), \quad (97)$$

where A_2 and A'_2 are given explicitly in Eqs. (72) and (77) respectively. Since $A'_2 > A_2$, the jump is nonnegative. Thus, at this critical point z_c , the rate function $\Phi(z)$ is nonanalytic

with a discontinuous second derivative. Hence, this corresponds to a second order phase transition.

It is interesting to compare the locations of z_{\min} , where $\Phi(z)$ reaches its global minimum, and the critical point z_c , at which $\Phi(z)$ is nonanalytic. This is best understood in terms of the phase diagram in the (λ, ρ) plane in Fig. 4. When $z \rightarrow z_{\min}$, we have seen that it corresponds to approaching $\lambda = 0$ along a horizontal axis corresponding to a fixed ρ . On the other hand, when z approaches z_c , it corresponds to λ approaching λ_c along the same horizontal axis. Thus, as long as $\lambda_c > 0$, we must have $z_c < z_{\min}$. On the other hand, if $\lambda_c < 0$, then $z_c > z_{\min}$. From the exact expressions of λ_c in Eq. (65) and $\rho_c(\beta)$ from Eq. (61), one sees that λ_c becomes 0 exactly when $\rho = \rho_c(\beta)$. For $\rho < \rho_c(\beta)$, one has $\lambda_c > 0$ and hence $z_{\min} < z_c$. In contrast, for $\rho > \rho_c(\beta)$, clearly $\lambda_c < 0$ and, hence, $z_c > z_{\min}$ (see Fig. 6 for a plot of $\Phi(z)$ in the two cases $\rho < \rho_c(\beta)$ and $\rho > \rho_c(\beta)$). Exactly at $\rho = \rho_c(\beta)$, where $\lambda_c = 0$, the two points z_{\min} and z_c coincide. In the (λ, ρ) plane, this special critical point corresponding to $\lambda_c = 0$ is shown by a red bullet, where, interestingly all the four phases F-F, F-C, C-F and C-C meet, indicating that this is a “multi-critical” point. The jump of the second derivative of $\Psi(z)$ also vanishes exactly at this multi-critical point $z = z_c$. In fact, one can show that the rate function $\Phi(z)$ becomes completely analytic around $z = z_{\min} = z_c$.

Let us make one interesting observation here. Consider the original system to be in the fluid phase where $\rho < \rho_c(\beta)$. If we stay in this fluid phase and do not change the density or the temperature, we do not have access to the condensed side. In other words, the partition function of the system has no information about the condensed side, unless one tunes the density or the temperature through the critical line $\rho_c(\beta) = \zeta(d)/\beta^d$. However, if one probes the rate function $\Phi(z)$ associated with the distribution of the moment of inertia $I = zV$, while staying completely inside the fluid phase, one finds the critical point $z_c < z_{\min}$ where the rate function undergoes a second order jump, signalling the existence of a condensed phase. In other words, we can set all the parameters of the system completely on the fluid side and yet access the signature of the condensed phase by choosing an appropriate observable (such as the moment of inertia here) and studying the rate function associated to its distribution. This is somewhat similar in spirit to devising a “tilted” Hamiltonian in importance sampling algorithms to access large deviation tails that describe rare events not captured by the typical statistics associated to a non-tilted Hamiltonian [44–46].

5 Conclusion

In this paper, we have studied, in all dimensions and at all temperature, the full probability distribution of the moment of inertia $I \propto \sum_{i=1}^N \vec{r}_i^2$ of N noninteracting trapped bosons in a harmonic potential $V(r) = (1/2)m\omega^2r^2$. In the thermodynamic limit $N \rightarrow \infty$ and $\omega \rightarrow 0$ with the product $\rho = N\omega^d$ fixed (that plays a role analogous to the density), and in dimension $d > 1$, the system undergoes a BEC phase transition, from a fluid phase at low density ($\rho < \rho_c(\beta)$) to a high density condensed phase (when $\rho > \rho_c(\beta)$) where $\rho_c(\beta) = \zeta(d)/\beta^d$, with β denoting the inverse temperature. We showed, that in the thermodynamic limit, the probability distribution $P_\beta(I, N)$ admits a large deviation form $P_\beta(I, N) \sim e^{-V\Phi(I/V)}$ where $V = \omega^{-d} \gg 1$, with a nontrivial rate function $\Phi(z)$ that we have computed analytically. The occurrence of the BEC transition in $d > 1$ introduces a singularity in the rate function $\Phi(z)$ at a critical value z_c , where its second derivative undergoes a discontinuous jump. One of the striking conclusions of our work is that, even if the actual system is in the fluid phase, i.e., when $\rho < \rho_c(\beta)$, by measuring the distribution

of I and analysing the singularity in the associated rate function, one can get a signal of the BEC transition in $d > 1$ without having to tune the actual density through $\rho = \rho_c(\beta)$.

In this paper, we focused on a specific linear statistics, namely $I \propto \sum_{i=1}^N \vec{r}_i^2$. In general, computing the full distribution of I is highly nontrivial even for noninteracting bosons, since one has to consider both quantum and thermal fluctuations, arising respectively from the Bose statistics and the finite temperature. However, for noninteracting bosons in a harmonic trap, we could perform this computation due to a nontrivial identity which we call a duality relation, that relates the cumulant generating function of I to the canonical partition function $Z(N, \beta)$. A first natural question is whether one can extend our calculations to non-harmonic traps, where such a duality relation is non-existent. We expect the associated rate function to depend explicitly on the potential. However, the singularity we found here in the rate function should also be present for a generic potential, provided it allows a BEC transition in the thermodynamic limit. Proving this is an interesting open problem. Furthermore, one can also ask whether such a singularity in the rate function shows up (for noninteracting bosons exhibiting a BEC transition) for other linear statistics of the form $\mathcal{L} = \sum_{i=1}^N f(\vec{r}_i)$ where $f(\vec{r})$ can be any arbitrary smooth function. For a generic $f(\vec{r})$, computing the full distribution of \mathcal{L} is highly nontrivial, even for noninteracting bosons in a harmonic trap. For the special case where $f(\vec{r}) = \vec{r}^2$, we could compute this distribution thanks to the nice duality relation that we derived in this paper. It would be interesting and challenging to see if similar duality relations can be derived for generic $f(\vec{r})$.

During the last years, there has been impressive numerical advances using importance sampling techniques to measure the rate functions associated with a probability distribution, up to very high precision. In particular, singularities in the rate function have been numerically detected in a variety of models (see [47, 48] for recent references). It would be interesting to see if the rate function computed analytically in this paper can be measured numerically.

Finally, the moment of inertia I is a rather natural observable whose statistics can hopefully be measured in cold atom experiments. In fact, in typical many-body quantum systems, exact results can sometimes be obtained only at zero temperature $T = 0$. At finite temperature, where most experimental data are available, very few exact results exist. Our work provides an exact finite temperature result for the statistics of I and hence, in principle, it would be possible to compare the future experimental data with our theoretical predictions.

6 Acknowledgments

SNM and GS acknowledges support from ANR Grant No. ANR-23- CE30-0020-01 EDIPS. MK acknowledges the support of the Department of Atomic Energy, Government of India, under project no. RTI4001.

A Derivation of the duality relation in d dimensions

In this appendix, we derive the duality relation stated in Eqs. (17) and (18). We consider the Hamiltonian of N noninteracting bosons in a harmonic trap in dimension d , namely

$$\hat{H}_N(m) = \sum_{i=1}^N \hat{h}_i(m) \quad \text{where} \quad \hat{h}_i(m) = \frac{\vec{p}_i^2}{2m} + \frac{1}{2}m\omega^2\vec{r}_i^2. \quad (98)$$

We want to compute the quantum average $\langle e^{-\lambda I} \rangle$, with $I = \omega^2 \sum_{i=1}^N \vec{r}_i^2$. For this we need to compute

$$\text{Tr} \left[e^{-\lambda \omega^2 \sum_{i=1}^N \vec{r}_i^2} e^{-\beta \hat{H}_N} \right] = \text{Tr} \left[e^{-\frac{\lambda}{2} \omega^2 \sum_{i=1}^N \vec{r}_i^2} e^{-\beta \hat{H}_N} e^{-\frac{\lambda}{2} \omega^2 \sum_{i=1}^N \vec{r}_i^2} \right] = \text{Tr} \left[\prod_i^N \hat{O}_i \right], \quad (99)$$

where $\hat{O}_i = e^{-\frac{\lambda}{2} \vec{r}_i^2} e^{-\beta \hat{h}_i(m)} e^{-\frac{\lambda}{2} \vec{r}_i^2}$. In the first equality, we have used the cyclicity of the trace while in the second equality we have used the fact that the bosons are noninteracting (and hence their Hamiltonians commute). Let us now consider a generic matrix element of the operator \hat{O}_i , namely

$$\langle \vec{y}_i | e^{-\frac{\lambda}{2} \vec{r}_i^2} e^{-\beta \hat{h}_i(m)} e^{-\frac{\lambda}{2} \vec{r}_i^2} | \vec{y}'_i \rangle = e^{-\frac{\lambda \omega^2}{2} (\vec{y}_i^2 + \vec{y}'_i^2)} \langle \vec{y}_i | e^{-\beta \hat{h}_i(m)} | \vec{y}'_i \rangle. \quad (100)$$

The matrix element on the right hand side of Eq. (100) factorises into d factors, one for each each component in d dimensions. Let us now recall the explicit expression of the propagator of the $1d$ quantum harmonic oscillator (in imaginary time), namely

$$\langle y | e^{-\beta \hat{h}(m)} | y' \rangle = \sqrt{\frac{m\omega}{2\pi\hbar \sinh(\beta\hbar\omega)}} \exp \left[-\frac{m\omega}{2\hbar \tanh(\beta\hbar\omega)} (y^2 + y'^2) + \frac{m\omega}{\hbar \sinh(\beta\hbar\omega)} (y y') \right]. \quad (101)$$

We next observe that the external factor $e^{-\frac{\lambda \omega^2}{2} (\vec{y}_i^2 + \vec{y}'_i^2)}$ on the right hand side of Eq. (100) can be absorbed in the quadratic form of the harmonic oscillator propagator in Eq. (101), leading us to rewrite Eq. (100) as

$$\langle \vec{y}_i | e^{-\frac{\lambda}{2} \vec{r}_i^2} e^{-\beta \hat{h}_i(m)} e^{-\frac{\lambda}{2} \vec{r}_i^2} | \vec{y}'_i \rangle = \langle \vec{y}_i | e^{-\tilde{\beta} \hat{h}_i(\tilde{m})} | \vec{y}'_i \rangle \quad (102)$$

in terms of renormalised parameters \tilde{m} and $\tilde{\beta}$

$$\tilde{m} = m \frac{\sinh(\tilde{\beta}\hbar\omega)}{\sinh(\beta\hbar\omega)}, \quad (103)$$

$$\cosh(\tilde{\beta}\hbar\omega) = \cosh(\beta\hbar\omega) + \lambda \frac{\hbar\omega}{m} \sinh(\beta\hbar\omega). \quad (104)$$

Therefore, using (99) together with (102) one has the key relation

$$\langle e^{-\lambda \omega^2 \sum_{i=1}^N \vec{r}_i^2} \rangle = \frac{1}{Z(N, \beta)} \text{Tr} \left[e^{-\lambda \omega^2 \sum_{i=1}^N \vec{r}_i^2} e^{-\beta \hat{H}_N} \right] = \frac{Z(N, \tilde{\beta})}{Z(N, \beta)}, \quad (105)$$

with

$$Z(N, \beta) = \text{Tr} \left[e^{-\beta \hat{H}_N(m)} \right]. \quad (106)$$

Note also that this relation gives the Laplace transform of $P(I, N)$ since

$$\tilde{P}(\lambda, N) = \int_0^\infty e^{-\lambda I} P(I, N) dI = \langle e^{-\lambda \omega^2 \sum_{i=1}^N \vec{r}_i^2} \rangle. \quad (107)$$

B Computation of the mean and the variance of I

We first recall the relation

$$\cosh(\tilde{\beta}(\lambda)\hbar\omega) = \cosh(\beta\hbar\omega) + \lambda\hbar\omega \sinh(\beta\hbar\omega). \quad (108)$$

Taking derivative with respect to λ one gets

$$\frac{\partial\tilde{\beta}(\lambda)}{\partial\lambda} = \frac{\sinh(\beta\hbar\omega)}{\sinh(\tilde{\beta}(\lambda)\hbar\omega)}. \quad (109)$$

Taking one more derivative with respect to λ and using the chain rule $\partial_\lambda = (\partial\tilde{\beta}/\partial\lambda)\partial_{\tilde{\beta}}$ gives

$$\frac{\partial^2\tilde{\beta}}{\partial\lambda^2} = -\hbar\omega \coth(\tilde{\beta}(\lambda)\hbar\omega) \frac{\sinh^2(\beta\hbar\omega)}{\sinh^2(\tilde{\beta}(\lambda)\hbar\omega)}. \quad (110)$$

Next we recall from Eq. (17) that the cumulant generating function of I is given by

$$\langle e^{-\lambda I} \rangle = \frac{Z(N, \tilde{\beta}(\lambda))}{Z(N, \beta)}. \quad (111)$$

Taking derivative with respect to λ and setting $\lambda = 0$ gives the expression for $\langle I \rangle$

$$\langle I \rangle = -\frac{\partial}{\partial\lambda} \langle e^{-\lambda I} \rangle \Big|_{\lambda=0} = -\frac{\partial}{\partial\tilde{\beta}} \left[\frac{Z(N, \tilde{\beta}(\lambda))}{Z(N, \beta)} \right] \frac{\partial\tilde{\beta}(\lambda)}{\partial\lambda} \Big|_{\lambda=0} \quad (112)$$

Using the relation in Eq. (109) for $\lambda = 0$ and $\tilde{\beta}(\lambda = 0) = \beta$ then gives

$$\langle I \rangle = -\frac{\partial \ln Z(N, \beta)}{\partial\beta}. \quad (113)$$

We now compute the variance $\text{Var}(I)$ which can be obtained from the cumulant generating function as

$$\text{Var}(I) = \frac{\partial^2}{\partial\lambda^2} \ln \langle e^{-\lambda I} \rangle \Big|_{\lambda=0}. \quad (114)$$

Using the relation in Eq. (111) one finds

$$\text{Var}(I) = \frac{\partial^2}{\partial\lambda^2} \left[\ln Z(N, \tilde{\beta}(\lambda)) \right] \Big|_{\lambda=0}. \quad (115)$$

Using again the chain rule $\partial_\lambda = (\partial\tilde{\beta}/\partial\lambda)\partial_{\tilde{\beta}}$ we then find

$$\text{Var}(I) = \frac{\partial^2}{\partial\tilde{\beta}^2} \left[\ln Z(N, \tilde{\beta}) \right] \left(\frac{\partial\tilde{\beta}}{\partial\lambda} \right)^2 \Big|_{\lambda=0} + \frac{\partial}{\partial\tilde{\beta}} \left[\ln Z(N, \tilde{\beta}) \right] \frac{\partial^2\tilde{\beta}}{\partial\lambda^2} \Big|_{\lambda=0} \quad (116)$$

Putting together the results from Eqs. (109), (110) and (113) one gets

$$\text{Var}(I) = \langle I^2 \rangle - \langle I \rangle^2 = \left[\frac{\partial^2 \ln Z}{\partial\beta^2} + \hbar\omega \coth(\beta\hbar\omega) \langle I \rangle \right]. \quad (117)$$

C The computation of a multidimensional integral

In this Appendix we compute the integral in Eq. (26), namely

$$\rho = \frac{1}{\beta^d} \int_{>} d\vec{k} \frac{1}{e^{s^* + \sum_{i=1}^d k_i} - 1}. \quad (118)$$

We first rewrite the integral as

$$\rho = \frac{1}{\beta^d} \int_0^\infty dq \int_{>} d\vec{k} \frac{1}{e^{s^* + q - 1}} \delta \left(q - \sum_{i=1}^d k_i \right). \quad (119)$$

We then perform first the integral over \vec{k} as follows. We define

$$I(q) = \int_{>} d\vec{k} \delta \left(q - \sum_{i=1}^d k_i \right). \quad (120)$$

Taking the Laplace transform with respect to q decouples the integral into d separate one-dimensional integrals, leading to

$$\int_0^\infty e^{-sq} I(q) dq = \frac{1}{s^d}. \quad (121)$$

Inverting the Laplace transform trivially we get

$$I(q) = \frac{1}{\Gamma(d)} q^{d-1}. \quad (122)$$

Substituting Eq. (122) in Eq. (119) gives

$$\tilde{\rho} = \rho \beta^d = \frac{1}{\Gamma(d)} \int_0^\infty dq q^{d-1} \frac{1}{e^{s^* + q} - 1}. \quad (123)$$

Now, expanding the integrand in powers of e^{-q} and integrating term by term gives the result in Eq. (27).

References

- [1] I. Bloch, J. Dalibard, W. Zwerger, *Many-body physics with ultracold gases*, Rev. Mod. Phys. **80**, 885 (2008), doi:10.1103/RevModPhys.80.885
- [2] S. Nascimbène, N. Navon, F. Chevy, C. Salomon, *The equation of state of ultracold Bose and Fermi gases: a few examples*, New J. Phys. **12**, 103026 (2010), doi:10.1088/1367-2630/12/10/103026
- [3] L. W. Cheuk, M. A. Nichols, M. Okan, T. Gersdorf, R. Vinay, W. Bakr, T. Lompe, M. Zwierlein, *Quantum-gas microscope for fermionic atoms*, Phys. Rev. Lett. **114**, 193001 (2015), doi:10.1103/PhysRevLett.114.193001
- [4] E. Haller, J. Hudson, A. Kelly, D. A. Cotta, B. Peaudecerf, G. D. Bruce, S. Kuhr, *Single-atom imaging of fermions in a quantum-gas microscope*, Nat. Phys. **11**, 738 (2015), doi:10.1038/nphys3403

[5] M. F. Parsons, F. Huber, A. Masurenko, C. S. Chiu, W. Setiawan, K. Wooley-Brown, S. Blatt, M. Greiner, *Site-resolved imaging of fermionic ^6Li in an optical lattice*, Phys. Rev. Lett. **114**, 213002 (2015), doi:10.1103/PhysRevLett.114.213002

[6] B. Mukherjee, Z. Yan, P. B. Patel, Z. Hadzibabic, T. Yefsah, J. Struck, M. W. Zwierlein, *Homogeneous atomic Fermi gases*, Phys. Rev. Lett. **118**, 123401 (2017), doi:10.1103/PhysRevLett.118.123401

[7] M. Anderson, J. Ensher, M. Matthews, C. Wieman, E. Cornell, *Observation of Bose-Einstein condensation in a dilute atomic vapor*, Science **269**, 198 (1995), doi:10.1126/science.269.5221.198

[8] K. Davis, M. O. Mewes, M. Andrews, N. van Druten, D. Durfee, D. Kurn, W. Ketterle, *Bose-Einstein condensation in a gas of sodium atoms*, Phys. Rev. Lett. **75**, 3969 (1995), doi:10.1103/PhysRevLett.75.3969

[9] C. Bradley, C. Sackett, J. Tollett, R. Hulet, *Evidence of Bose-Einstein condensation in an atomic gas with attractive interactions*, Phys. Rev. Lett. **75**, 1687 (1995), doi:10.1103/PhysRevLett.75.1687

[10] E. A. Cornell, C. E. Wieman, *Nobel Lecture: Bose-Einstein condensation in a dilute gas, the first 70 years and some recent experiments*, Rev. Mod. Phys. **74**, 875 (2002), doi:10.1103/RevModPhys.74.875

[11] A. J. Leggett, *Bose-Einstein condensation in the alkali gases: Some fundamental concepts*, Rev. Mod. Phys. **73**, 307 (2001), doi:10.1103/RevModPhys.73.307

[12] F. Dalfovo, S. Giorgini, L. P. Pitaevskii, S. Stringari, *Theory of Bose-Einstein condensation in trapped gases*, Rev. Mod. Phys. **71**, 463 (1999), doi:10.1103/RevModPhys.71.463

[13] J. Verstraten, K. Dai, M. Dixmerias, B. Peaudecerf, T. de Jongh, and T. Yefsah, *In Situ Imaging of a Single-Atom Wave Packet in Continuous Space*, Phys. Rev. Lett. **134**, 083403 (2025), doi:10.1103/PhysRevLett.134.083403

[14] T. de Jongh, J. Verstraten, M. Dixmerias, C. Daix, B. Peaudecerf, and T. Yefsah, *Quantum gas microscopy of fermions in the continuum*, Phys. Rev. Lett. **134**, 183403 (2025), doi:10.1103/PhysRevLett.134.183403

[15] R. Yao, S. Chi, M. Wang, R. J. Fletcher, and M. Zwierlein, *Measuring pair correlations in Bose and Fermi gases via atom-resolved microscopy*, Phys. Rev. Lett. **134**, 183402 (2025), doi:10.1103/PhysRevLett.134.183402

[16] M. Dixmerias, G. Del Vecchio Del Vecchio, C. Daix, J. Verstraten, T. de Jongh, B. Peaudecerf, P. Le Doussal, G. Schehr, T. Yefsah, *Universal Random Matrix Behavior of a Fermionic Quantum Gas*, preprint arXiv:2510.25735, doi:10.48550/arXiv.2510.25735

[17] T. Gericke, P. Würtz, D. Reitz, T. Langen, H. Ott, *High-resolution scanning electron microscopy of an ultracold quantum gas*, Nat. Phys. **4** 949 (2008), doi:10.1038/nphys1102

[18] Y. Morita, K. Yoshioka, M. Kuwata-Gonokami, *Observation of Bose-Einstein condensates of excitons in a bulk semiconductor*, Nat. Commun. **13**, 5388 (2022), doi:10.1038/s41467-022-33103-4

[19] R. M. Ziff, G. E. Uhlenbeck, M. Kac, *The ideal Bose-Einstein gas, revisited*, Phys. Rep. **32**, 169 (1977), doi:10.1016/0370-1573(77)90052-7

[20] K. Huang, *Statistical mechanics*, John Wiley & Sons (2008).

[21] R. K. Pathria, *Statistical Mechanics: International Series of Monographs in Natural Philosophy* (Vol. 45), Elsevier (2017).

[22] D. S. Dean, P. Le Doussal, S. N. Majumdar, G. Schehr, *Noninteracting fermions at finite temperature in ad-dimensional trap: Universal correlations*, Phys. Rev. A, **94**, 063622 (2016), doi:10.1103/PhysRevA.94.063622

[23] D. S. Dean, P. Le Doussal, S. N. Majumdar, G. Schehr, *Statistics of the maximal distance and momentum in a trapped Fermi gas at low temperature*, J. Stat. Mech. 063301 (2017), doi:10.1088/1742-5468/aa6dda

[24] B. Lacroix-A-Chez-Toine, S. N. Majumdar, G. Schehr, *Rotating trapped fermions in two dimensions and the complex Ginibre ensemble: Exact results for the entanglement entropy and number variance*, Phys. Rev. A **99**, 021602 (2019), doi:10.1103/PhysRevA.99.021602

[25] G. Gouraud, P. Le Doussal, G. Schehr, *Hole probability for noninteracting fermions in a d-dimensional trap*, Europhys. Lett. **137**, 50003 (2022), doi:10.1209/0295-5075/ac4aca

[26] D. S. Dean, P. Le Doussal, S. N. Majumdar, G. Schehr, *Noninteracting fermions in a trap and random matrix theory*, J. Phys. A: Math. and Theor. **52**, 144006 (2019), doi:10.1088/1751-8121/ab098d

[27] J. Grela, S. N. Majumdar, G. Schehr, *Kinetic energy of a trapped Fermi gas at finite temperature*, Phys. Rev. Lett. **119**, 130601 (2017), doi:10.1103/PhysRevLett.119.130601

[28] W. S. Bakr, J. I. Gillen, A. Peng, S. Folling, M. Greiner, *A quantum gas microscope for detecting single atoms in a Hubbard-regime optical lattice*, Nature **462**, 74 (2009), doi:10.1038/nature08482

[29] W. S. Bakr, A. Peng, M. E. Tai, R. Ma, J. Simon, J. I. Gillen, S. Folling, L. Pollet, M. Greiner, *Probing the Superfluid-to-Mott Insulator Transition at the Single- Atom Level*, Science **329**, 547 (2010), doi:10.1126/science.1192368

[30] J. F. Sherson, C. Weitenberg, M. Endres, M. Cheneau, I. Bloch, S. Kuhr, *Single-atom-resolved fluorescence imaging of an atomic Mott insulator*, Nature **467**, 68 (2010), doi:10.1038/nature09378

[31] C. Gross, W. S. Bakr, *Quantum gas microscopy for single atom and spin detection*, Nat. Phys. **17** 1316 (2021), doi:10.1038/s41567-021-01370-5

[32] S. Buob, J. Hoschele, V. Makhlov, A. Rubio-Abadal, L. Tarruell, *A Strontium Quantum-Gas Microscope*, Phys. Rev. X Quant. **5** 020316 (2024), doi:10.1103/PRXQuantum.5.020316

[33] K. Damle, T. Senthil, S. N. Majumdar, S. Sachdev, *Phase transition of a Bose gas in a harmonic potential*, Europhys. Lett. **36**, 7 (1996), doi:10.1209/epl/i1996-00179-4

[34] A. Crisanti, L. Salasnich, A. Sarracino, M. Zannetti, *Canonical vs. Grand Canonical Ensemble for Bosonic Gases under Harmonic Confinement*, Entropy **26**, 367 (2024), doi:10.3390/e26050367

[35] M. R. Evans, T. Hanney, *Nonequilibrium statistical mechanics of the zero-range process and related models*, J. Phys. A: Math. Gen. **38**, R195 (2005), doi:10.1088/0305-4470/38/19/R01

[36] S. N. Majumdar, *Real-space condensation in stochastic mass transport models* in *Exact Methods in Low-Dimensional Statistical Physics and Quantum Computing* (Les Houches 2008, Session LXXXIX), Oxford University Press, Oxford, 407 (2010).

[37] S. N. Majumdar, M. R. Evans, R. K. P. Zia, *Nature of the condensate in mass transport models*, Phys. Rev. Lett. **94**, 180601 (2005), doi:10.1103/PhysRevLett.94.180601

[38] M. R. Evans, S. N. Majumdar, R. K. P. Zia, *Canonical analysis of condensation in factorised steady states*, J. Stat. Phys. **123**, 357 (2006), doi:10.1007/s10955-006-9046-6

[39] G. Gradenigo, S. N. Majumdar, *A first-order dynamical transition in the displacement distribution of a driven run-and-tumble particle*, J. Stat. Mech. 053206 (2019), doi:10.1088/1742-5468/ab11be

[40] F. Mori, G. Gradenigo, S. N. Majumdar, *First-order condensation transition in the position distribution of a run-and-tumble particle in one dimension*, J. Stat. Mech. 103208 (2021), doi:10.1088/1742-5468/ac2899

[41] F. Mori, P. Le Doussal, S. N. Majumdar, G. Schehr, *Condensation transition in the late-time position of a run-and-tumble particle*, Phys. Rev. E **103**, 062134 (2021), doi:10.1088/1742-5468/ac2899

[42] G. Gradenigo, S. Iubini, R. Livi, S. N. Majumdar, *Localization transition in the discrete nonlinear Schrödinger equation: ensembles inequivalence and negative temperatures*, J. Stat. Mech. 023201 (2021), doi:10.1088/1742-5468/abda26

[43] G. Gradenigo, S. Iubini, R. Livi, S. N. Majumdar, *Condensation transition and ensemble inequivalence in the discrete nonlinear Schrödinger equation*, Eur. Phys. J. E **44**, 29 (2021), doi:10.1140/epje/s10189-021-00046-5

[44] A. K. Hartmann, *Sampling rare events: Statistics of local sequence alignments*, Phys. Rev. E **65**, 056102 (2002), doi:10.1103/PhysRevE.65.056102

[45] J. A. Bucklew, *Introduction to Rare Event Simulation* (Springer New York, NY, 2004).

[46] W. Krauth, *Statistical Mechanics Algorithms and Computations* (Cambridge University Press, Cambridge, 2006).

[47] I. N. Burenev, S. N. Majumdar, A. Rosso, *Importance Sampling for counting statistics in one-dimensional systems*, J. Chem. Phys. **161**, 054115 (2024), doi:10.1063/5.0221076

[48] P. Werner, A. K. Hartmann, *Numerical Estimation of Limiting Large-Deviation Rate Functions*, arXiv preprint arXiv:2412.04206 (2024), doi:10.48550/arXiv.2412.04206